Supplementary material related to the article

GALLOYL CARBOHYDRATES WITH ANTIANGIOGENIC ACTIVITY MEDIATED BY CAPILLARY MORPHOGENESIS GENE 2 (CMG2) PROTEIN BINDING

Elisa G.-Doyagüez[1,2#], Paula Carrero[1,¥,#], Andrés Madrona[1,γ], Patricia Rodriguez-Salamanca[1λ], Belén Martínez-Gualda[1,π], María-José Camarasa[1], María Luisa Jimeno[2], Philip R. Bennallack[3], Jordan G. Finnell[4,φ], Tsz Ming Tsang[4], Kenneth A. Christensen[4], Ana San-Félix[*1], Michael S. Rogers[*3]

[1]Instituto de Química Médica (IQM, CSIC), Madrid, Spain
[2]Centro de Química Orgánica "Lora-Tamayo" (CENQUIOR, CSIC), Madrid, Spain
[3]Vascular Biology Program, Boston Children's Hospital and Harvard Medical School, Boston, MA, USA
[4]Department of Chemistry and Biochemistry, Brigham Young University, Provo, UT, USA
[¥]Current address: Laboratorios Liconsa, S.A., Azuqueca de Henares - Guadalajara, Spain
[γ]Current address: Novartis Farmacéutica S.A., Barcelona, Spain
[π] Current address: Rega Institute for Medical Research, Laboratory of Medicinal Chemistry, Leuven, Belgium
[φ] Current address: Center for Alzheimer's and Neurodegenerative Diseases, University of Texas Southwestern Medical Center, Dallas, TX, USA
[λ] Current address: Instituto de Investigaciones Químicas, Sevilla, Spain

**Corresponding authors:*
Ana San-Félix: Tel: + 34 91 2587617, E-mail: anarosa@iqm.csic.es
Michael Rogers: Tel: +1-617-919-2252, E-mail: michael.rogers@tch.harvard.edu

Includes:

1. Structural assignments
2. Inhibitory effects of **4**, **7**, **8**, **13**, **19** and **29** with respect to PA-CMG2 inhibition. Dose-response curves determined by a FRET interaction assay
3. Selected ^{1}H and ^{13}C NMR spectra

1. *Structural assignments*

The structures of the novel carbohydrate derivatives were assigned by ^{1}H and ^{13}C NMR spectroscopic analysis. In the case of the gallic acid monosaccharide series, compounds **3-10**, the spectroscopic data were identical to those reported previously.[1]

For the novel 2,3,4-trihydroxybenzoyl monosaccharide and disaccharide compounds well-known NMR rules,[2] together with bidimensional NOESY and ROESY experiments and ^{13}C-^{1}H techniques (gHMBC[3] and gHSQC[4]) have been applied for the unequivocal assignment of the structures.

Table 1 showed all the chemical shifts and coupling constants observed for 2,3,4-trihydroxybenzoyl monosaccharides series.

Table 1. NMR data (chemical shifts and coupling constants) observed for 2,3,4-trihydroxybenzoyl monosaccharide series.

	13 α/β-D-Glc*p**	**15** α-D-Gal*f***	**18** α-D-Man*p*	**19** β-D-Man*p*	**22** α-D-Rib*p*	**23** β-D-Rib*p*
δ (ppm)						
C-1	91.76/93.97	95.85	92.65	92.13	90.71	93.84
C-2	71.95/72.45	77.38	70.27	70.72	68.22	68.88 or 69.07
C-3	72.12/74.28	75.47	71.35	72.47	68.99	67.73
C-4	70.17/ 70.75	80.68	66.60	67.25	67.41	68.88 or 69.07
C-5	72.23/74.20	71.60	72.44	73.90		64.76
C-6	63.89/64.09	63.95	62.69	62.98	-	-
H-1	6.85/6.39	6.80	6.57	6.53	6.56	6.57
H-2	5.70/5.75	5.94	5.93	6.08	5.76	5.62-5.70
H-3	6.20/6.08	6.26	5.98	5.92	6.15	6.01
H-4	5.82/5.75	4.79-4.85	6.16	6.05	5.60	5.62-5.70
H-5	4.50-4.70	5.85	4.52-4.68	4.49	4.13 (5_A), 4.45 (5_B)	4.21 (5_A), 4.46 (5_B)
H-6_A	4.50-4.70	4.65	4.52-4.68	4.62		
H-6_B	4.50-4.70	4.79-4.85	4.52-4.68	4.71		
$^{3}J_{HH}$ (Hz)						
$^{3}J_{1,2}$	3.7/7.9	4.8	1.9	1.1	3.9	2.7
$^{3}J_{2,3}$	9.9/9.6	6.4	3.2	3.2	3.5	3.9
$^{3}J_{3,4}$	9.9/9.6	6.4	10.2	9.9	4.0	3.9
$^{3}J_{4,5}$	9.9/9.3	3.6	10.1	9.9	4.2 ($^{3}J_{4,5A}$), 9.1 ($^{3}J_{4,5B}$)	3.5
$^{3}J_{5,6A}$	-	6.0	-	3.0	11.5 ($^{3}J_{5A,5B}$)	13.3 ($^{3}J_{5A,5B}$)
$^{3}J_{5,6B}$	-	5.6	-	2.5		
$^{2}J_{6A,6B}$	-	12.4	-	12.5		

**p: Pyranose form*
***f: Furanose form*

According to the NMR carbohydrate rules,[2] for pyranoses in a $^{4}C_1$ conformation, a large coupling constant ($J_{1,2}$ = 7-10 Hz) between the anomeric H1 and the H2 indicates that both protons are in an axial configuration, whereas if they are equatorial-axial the coupling constant is smaller ($J_{1,2}$ ~ 4 Hz) and for axial-equatorial or equatorial-equatorial oriented protons even smaller coupling constants are observed ($J_{1,2}$ < 2 Hz). Following these rules the glucopyranose derivative **13** were confirmed as an anomeric α/β mixture 1:2.

In the case of the galactose derivative **15**, the ^{13}C NMR spectrum shows that the chemical shifts are in agreement with those reported for a furanose with α configuration (α-Gal*f*) instead of a pyranose form (Table

1).[5-7] The multiplicity and *J* value of the H-3, $\hat{o}$ = 6.26 (t, *J* = 6.4 Hz, 1H, H-3) is also consistent with a furanose form. Moreover, the $J_{1,2}$ value obtained for this compound (4.8 Hz) is characteristic of a furanose (α-Gal*f)* configuration. Furanose conformation was corroborated using a bidimensional HMBC experiment. Thus, the 2D-HMBC spectrum (Figure 1) shows two intense correlation signals, between C-1/H-4 and C-4/H-1, only possible if the sugar is in the furanose form (C1 and C4 separated by three bonds).

Compound **15**

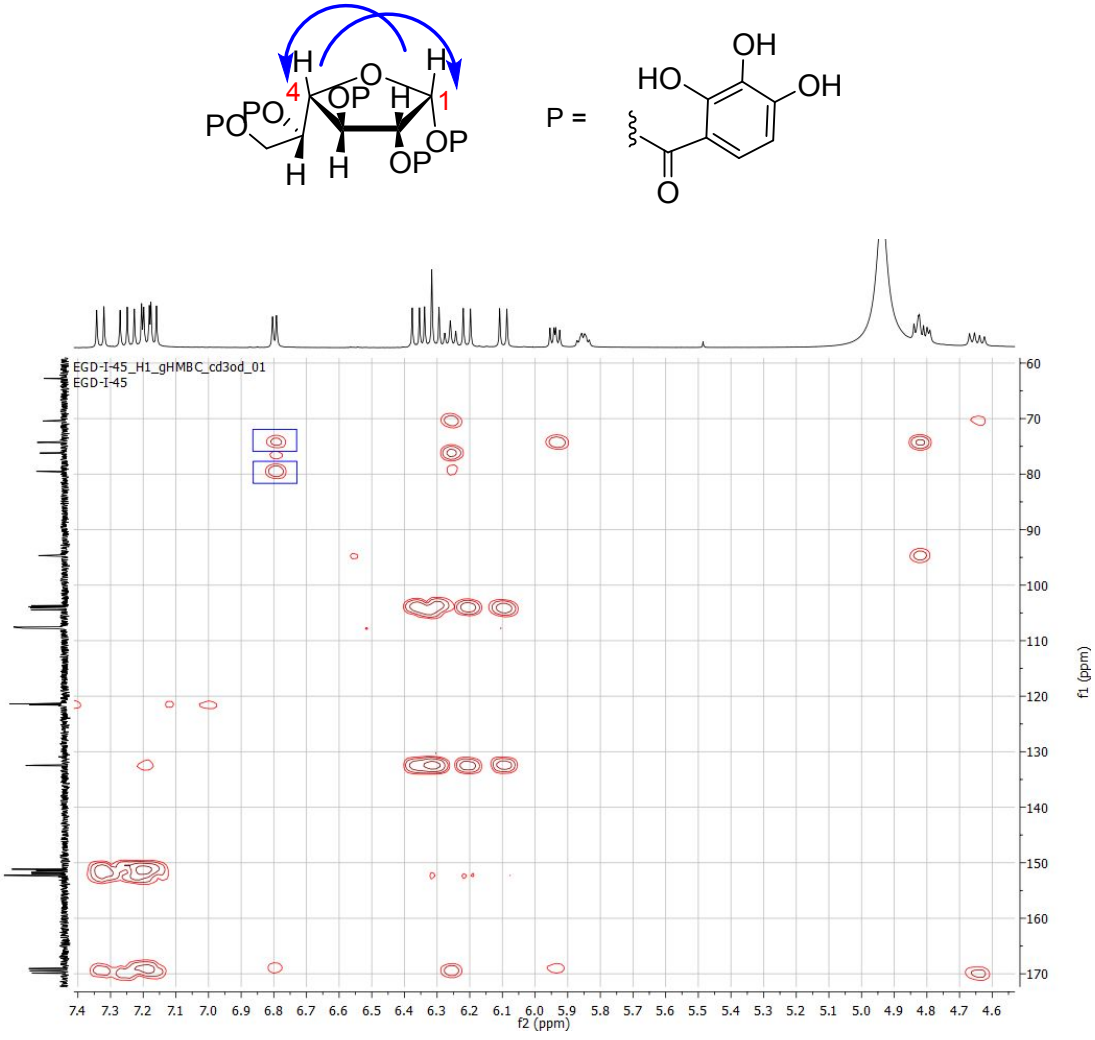

Figure 1. *Structural assignments and HMBC correlations observed for galactose derivative* ***15***

For mannose derivatives **18** and **19**, the $J_{1,2}$ values obtained were very similar (1.9 Hz and 1.1 Hz, respectively) and α and β assignment was not easy (Table 1).

In the HMBC spectrum for compound **18** a correlation between H-1 and C-3 was observed indicating that H-1 is situated in an equatorial position (α-configuration), giving the appropriate dihedral angle value (C1, C2 and C3 in W disposition) (Figure 2 left). However HMBC for **19** (β-configuration) did not show such correlation (Figure 2, right).

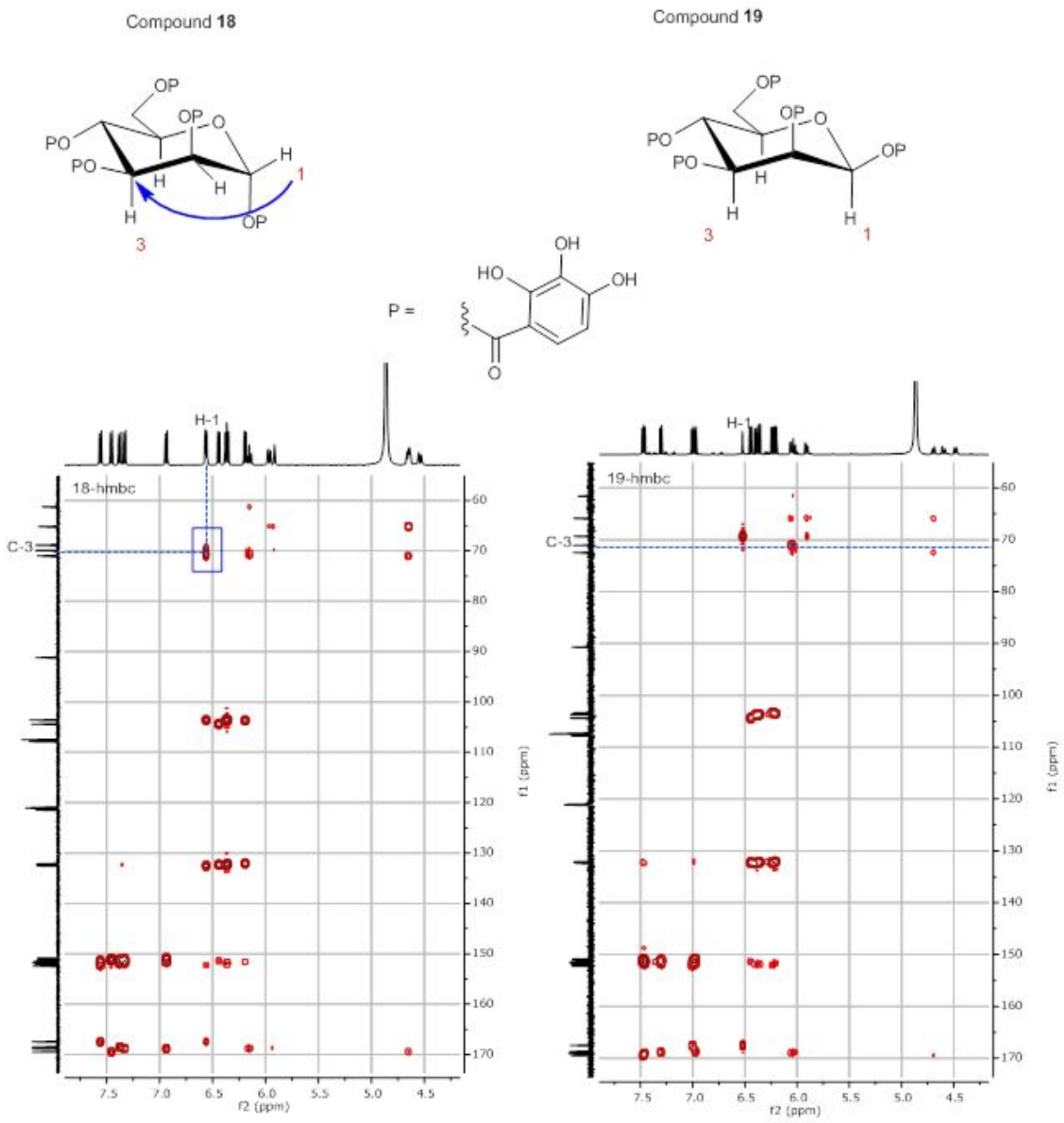

Figure 2. *Structural assignments and HMBC correlations observed for mannose derivatives* ***18*** *(left) and* ***19*** *(right)*

In the 2D-ROESY spectrum of **19** correlations H-1/H-3 and H-1/H-5 were observed. However, in compound **18**, H-1 only correlates with H-2 (Figure 3). These data also support the proposed structures.

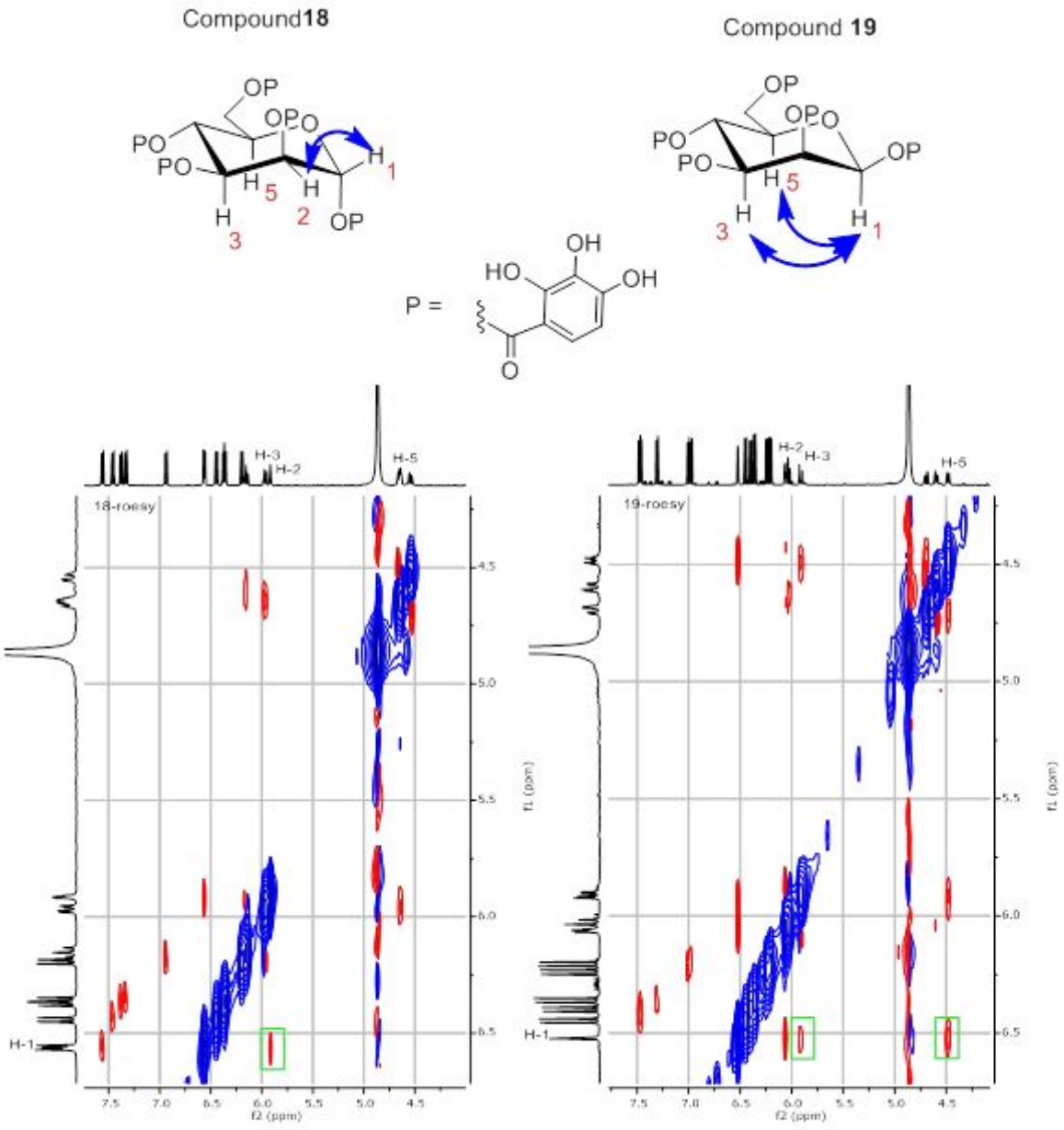

Figure 3. *Structural assignments and ROESY correlations observed for mannose derivatives* ***18*** *and* ***19***

The $^4C_1$ conformation and α configuration of the ribopyranose derivative **22** was supported by a small coupling constant ($J_{1,2}$ = 3.9 Hz) (Table 1). However the smaller coupling constant observed for **23** ($J_{1,2}$ = 2.7 Hz) does not match with a $^4C_1$ β configuration. For this compound gHMBC experiments (Figure 4) revealed two long-range correlations between the H1 proton (δ 6.57 ppm) and the C3 (δ 67.73 ppm) and C5 carbons (δ 64.76 ppm). These data allowed to propose for **23** a different conformational state ($^1C_4$) and a β configuration.

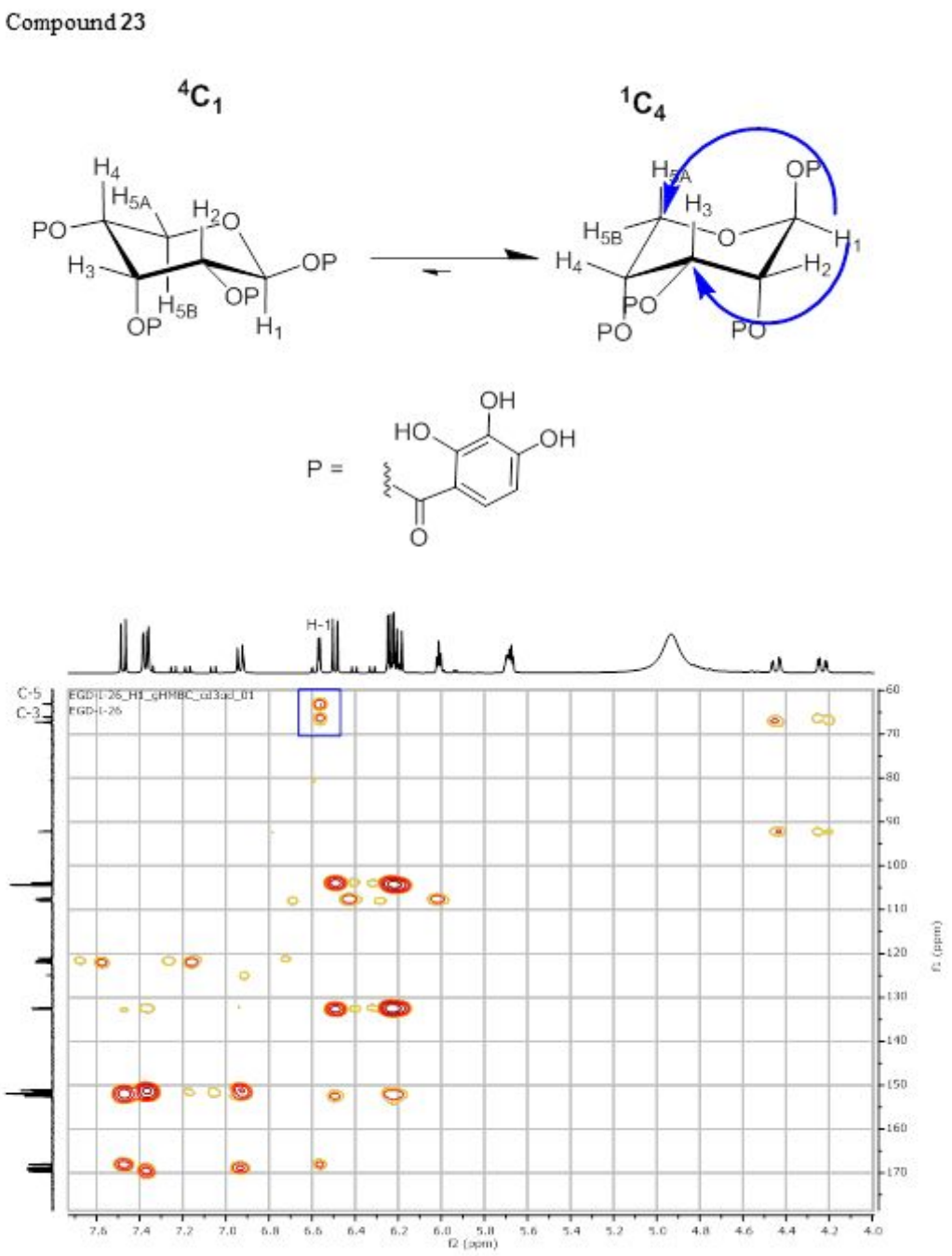

Figure 4. *Structural assignments and HMBC correlation, observed for ribose derivative* ***23***

For the disaccharide compounds **25, 27, 29** and **31**, homonuclear COSY spectra were used in the identification of individual monosaccharide residues.

In the galloyl maltose derivative **25**, a coupling constant $J_{1,2}$ = 3.9 Hz allowed the unambigous assignment of a β configuration for residue B (numbered 1-6), while a coupling constant $J_{1,2}$ = 8.3 Hz corroborates the α configuration of residue A (numbered 1'-6'). The same was observed for the 2,3,4-trihydroxybenzoyl maltose derivative **29**.

Compound **25**

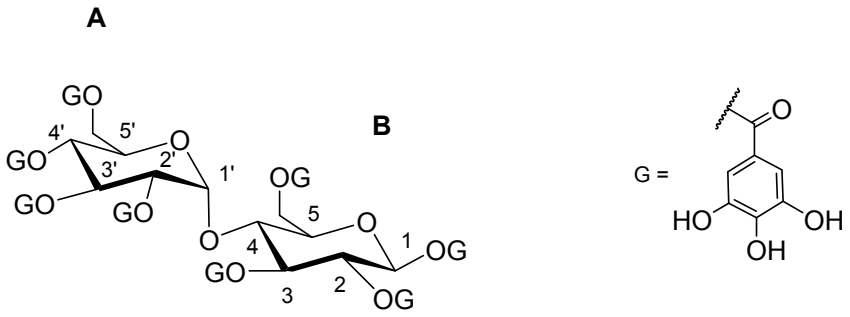

Figure 5. *Structure of compound **25** as a representative example of a maltose derivative*

In trehalose derivatives, **27** and **31,** two coupling constants $J_{1,2}$ = 3.7 Hz allowed the unambigous assignment of a α,α configuration for the two sugar residues.

Compound **27**

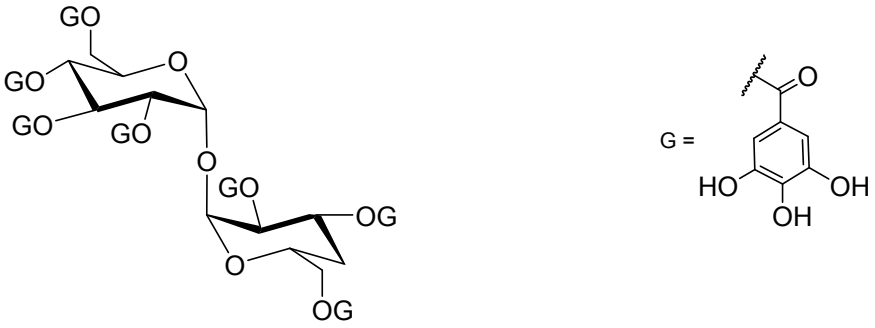

Figure 6. *Structure of compound **27** as a representative example of a trehalose derivative*

2. Inhibitory effects of 4, 7, 8, 13, 19 and 29 with respect to PA-CMG2 inhibition. Dose-response curves determined by a FRET interaction assay

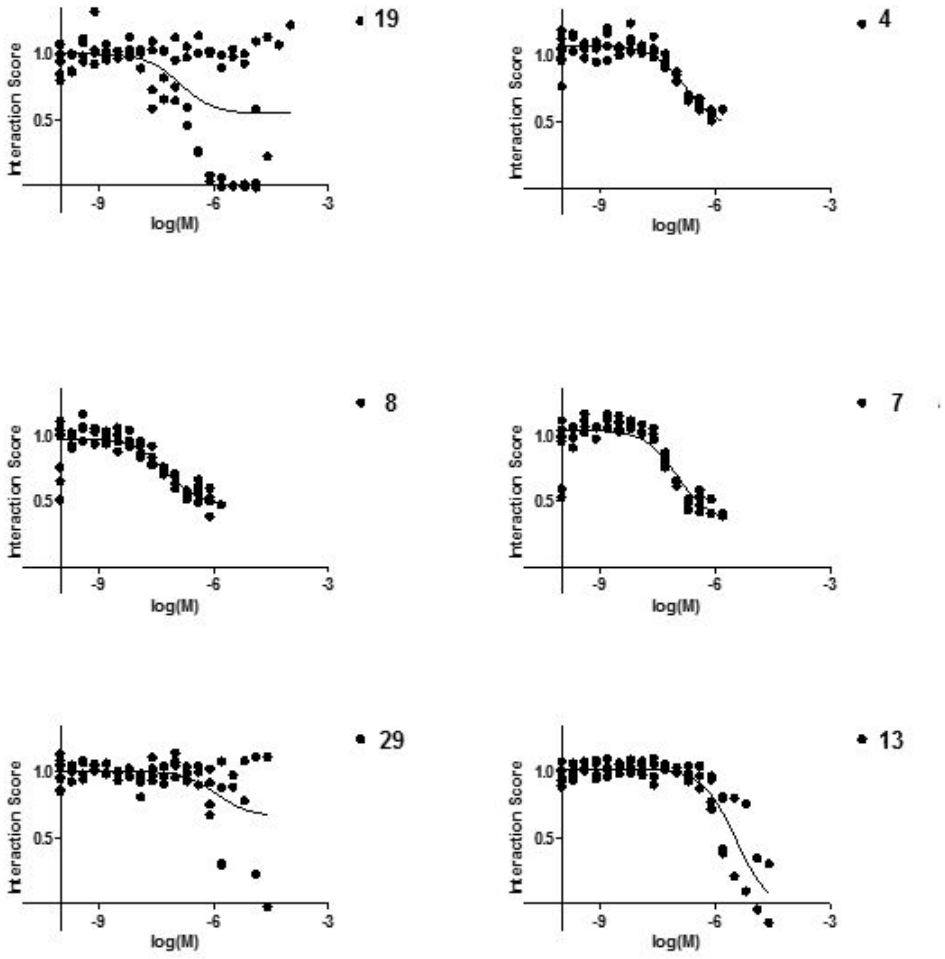

***Figure** 7. Dose-response curves for synthesized compounds* **4, 7**, **8, 13, 19** and **29**

Interaction score represents the fraction of control interaction exhibited in a given well. Curves are best-fit binding isotherms with Hill coefficient of 1.

3. Selected ^{1}H and ^{13}C NMR spectra

Compound 12 (^{1}H-NMR)

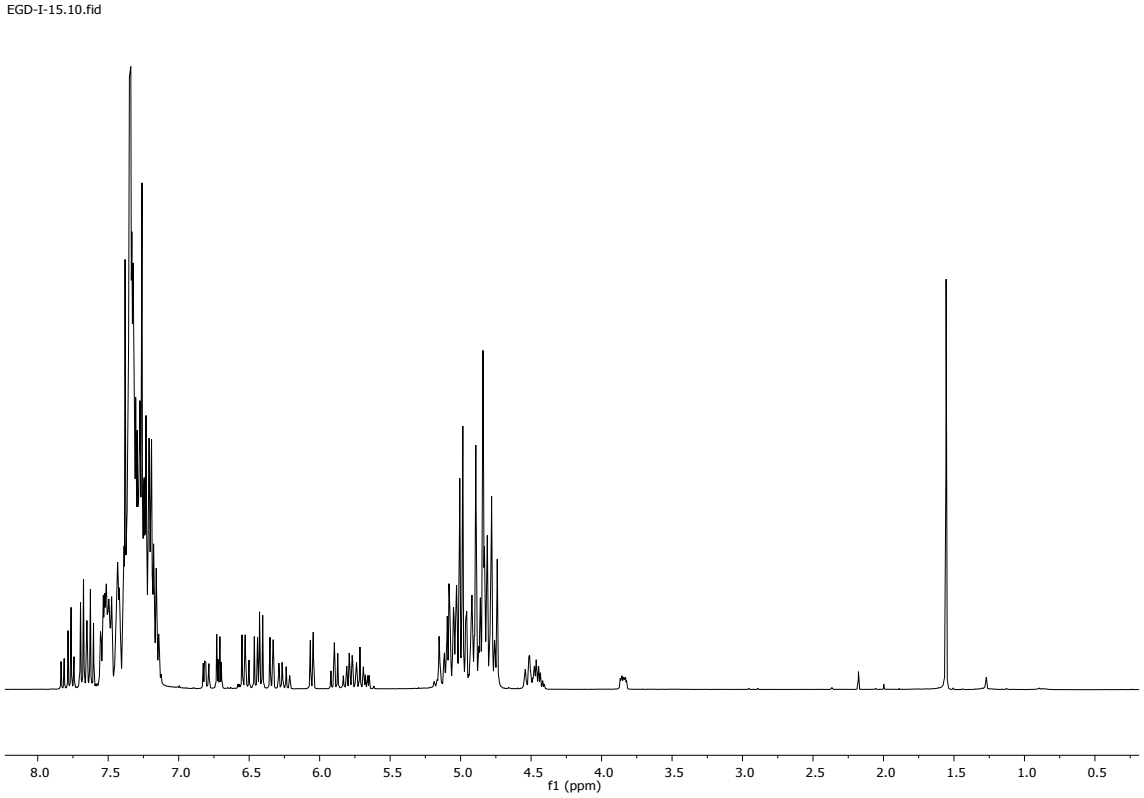

Compound 12 (^{13}C-NMR)

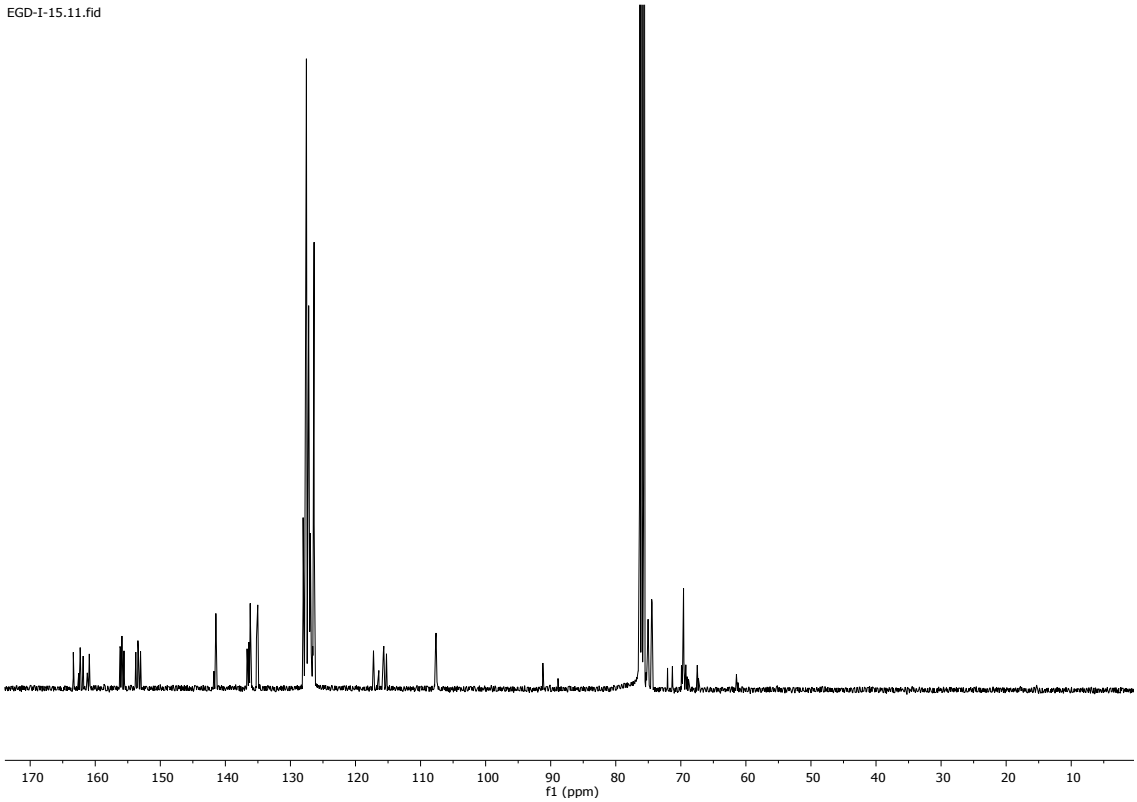

Compound 13 (^{1}H- NMR)

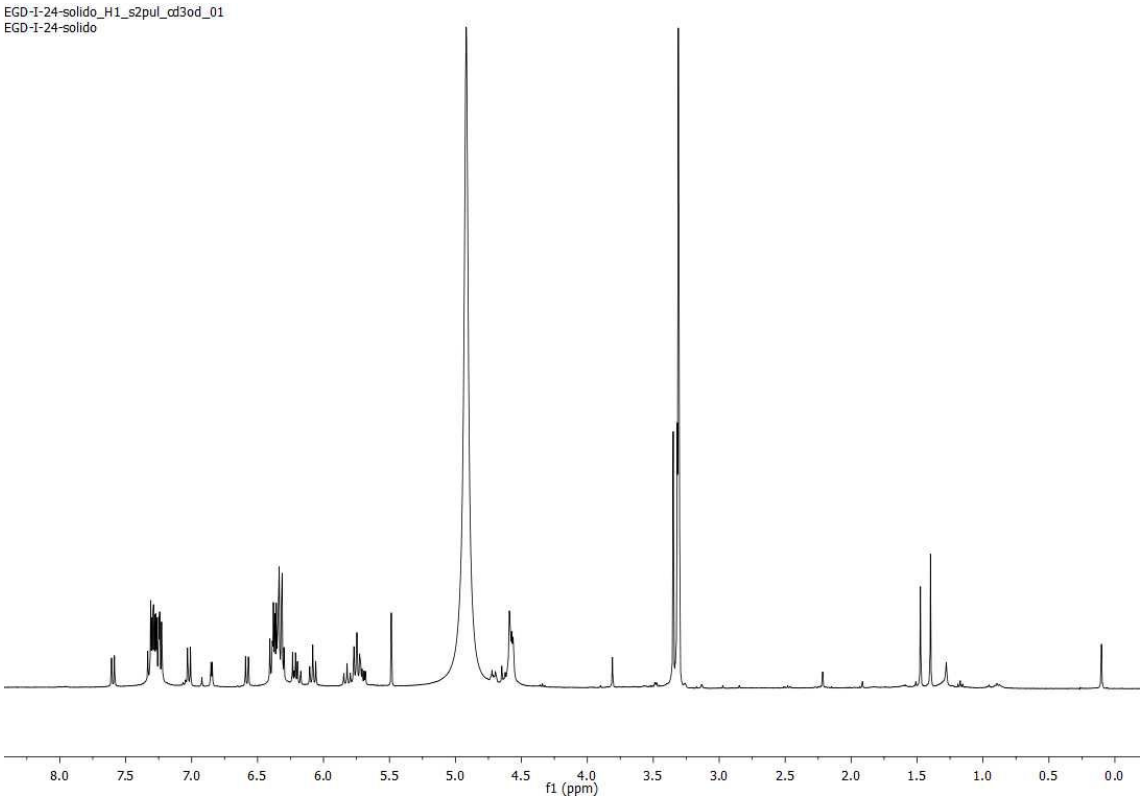

Compound 13 (^{13}C-NMR)

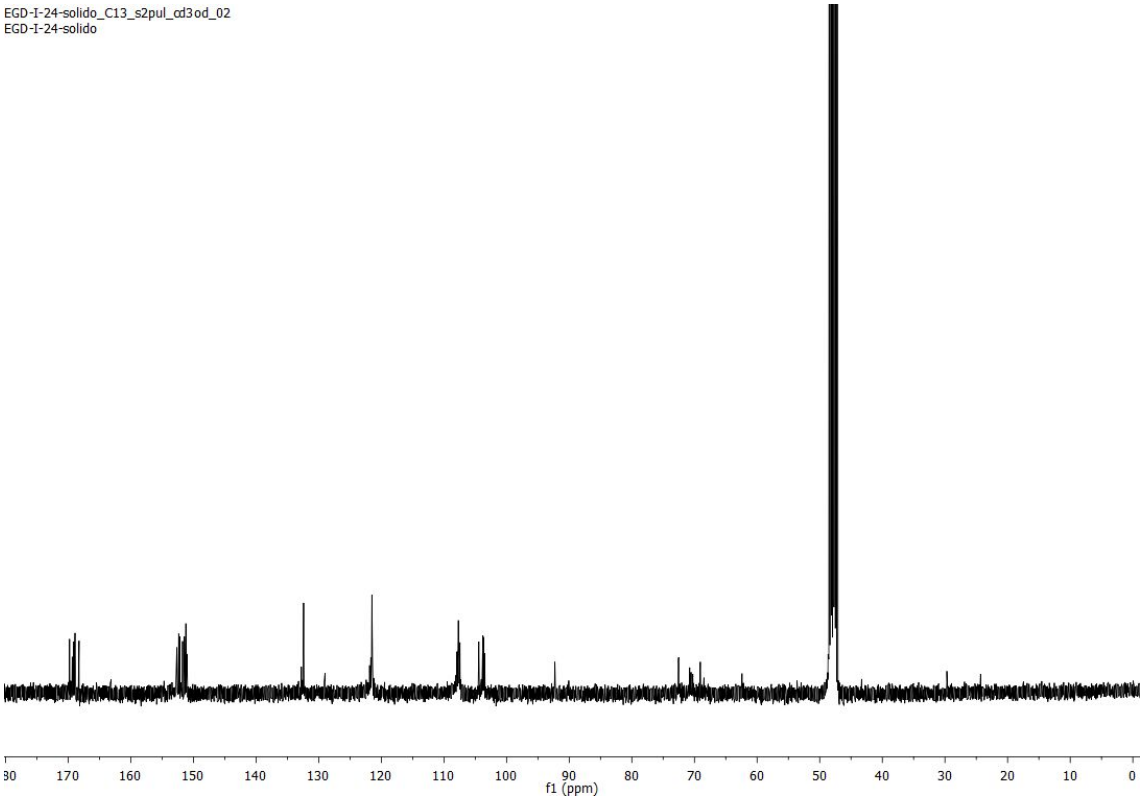

Compound 14 (^{1}H- NMR)

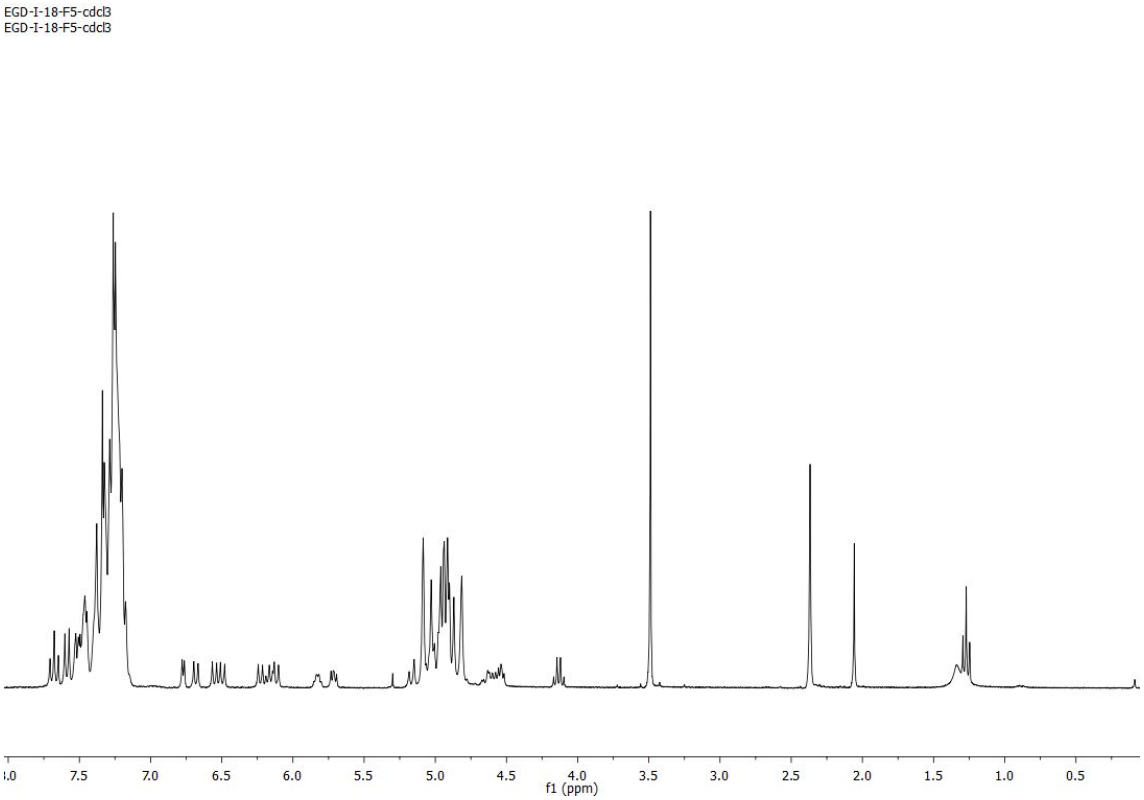

Compound 15 (^{1}H- NMR)

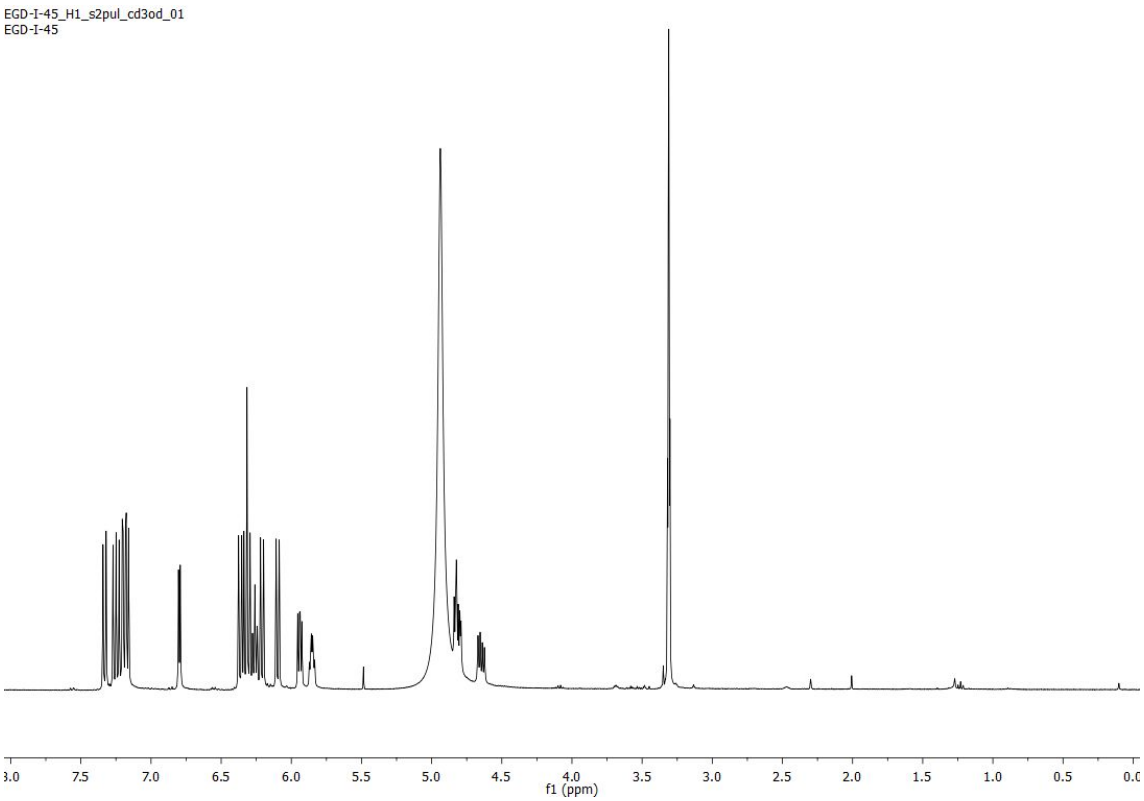

Compound 15 (^{13}C- NMR)

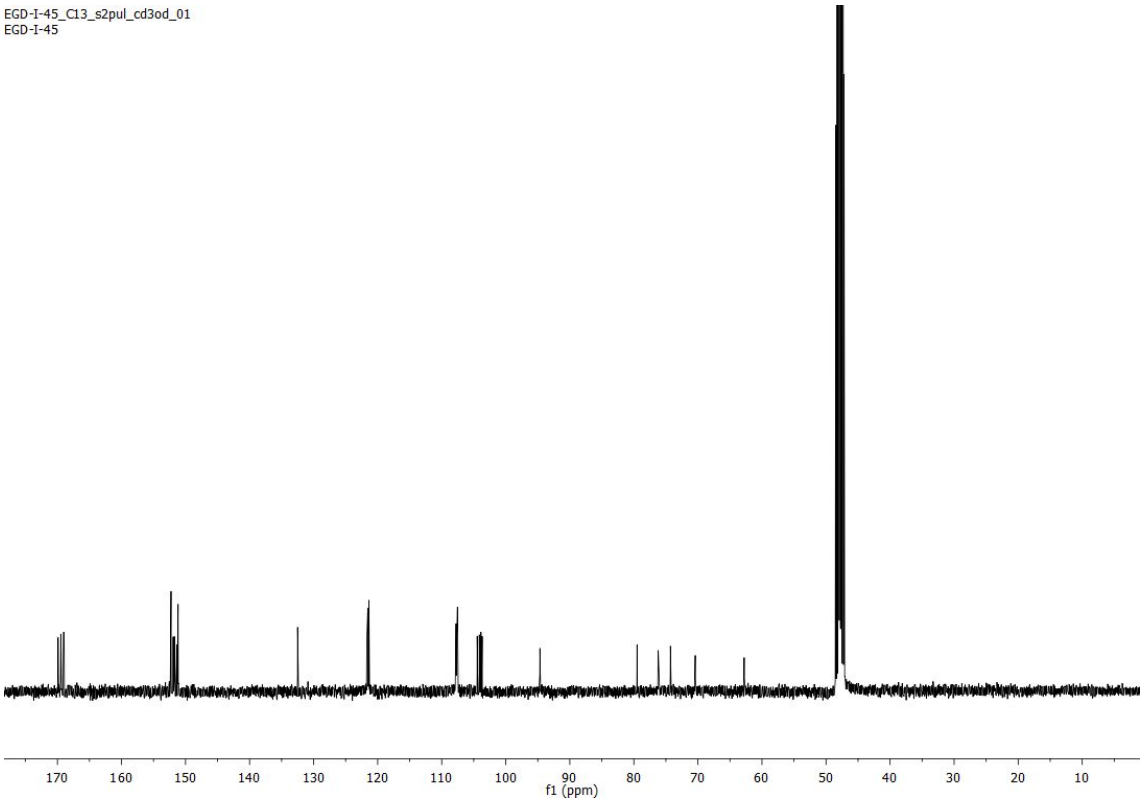

Compound 16 (^{1}H- NMR)

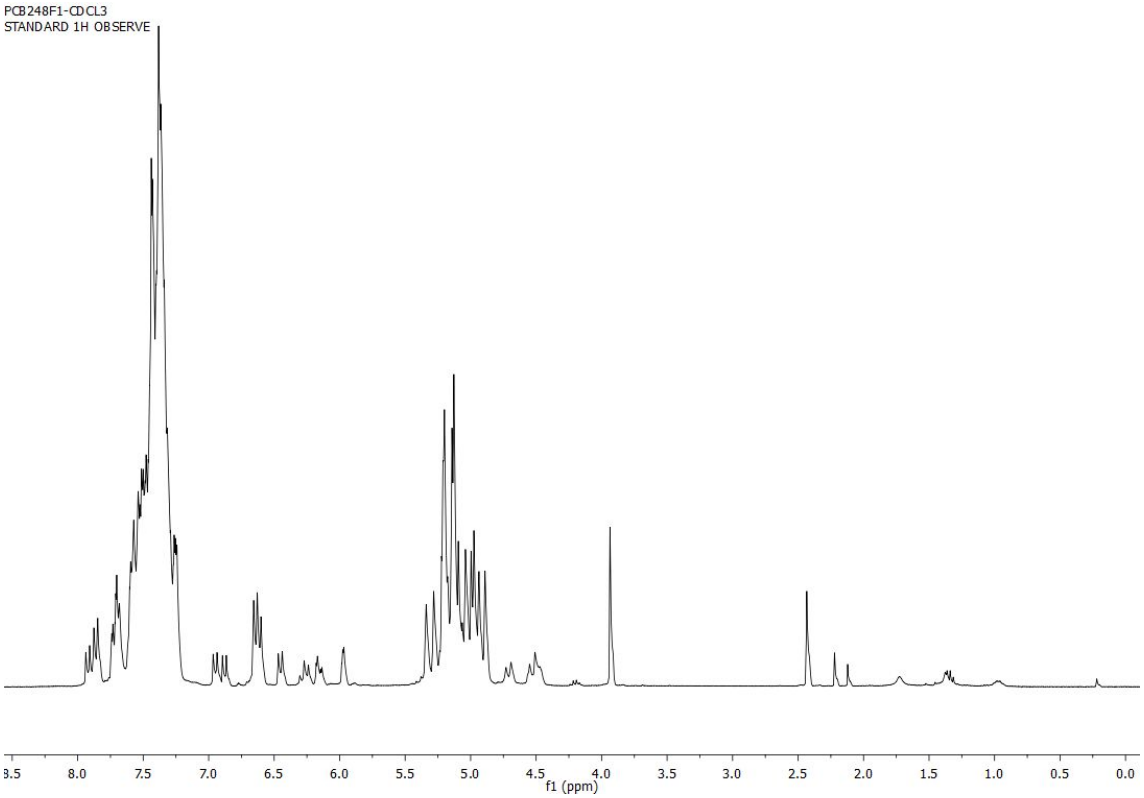

Compound 16 (^{13}C- NMR)

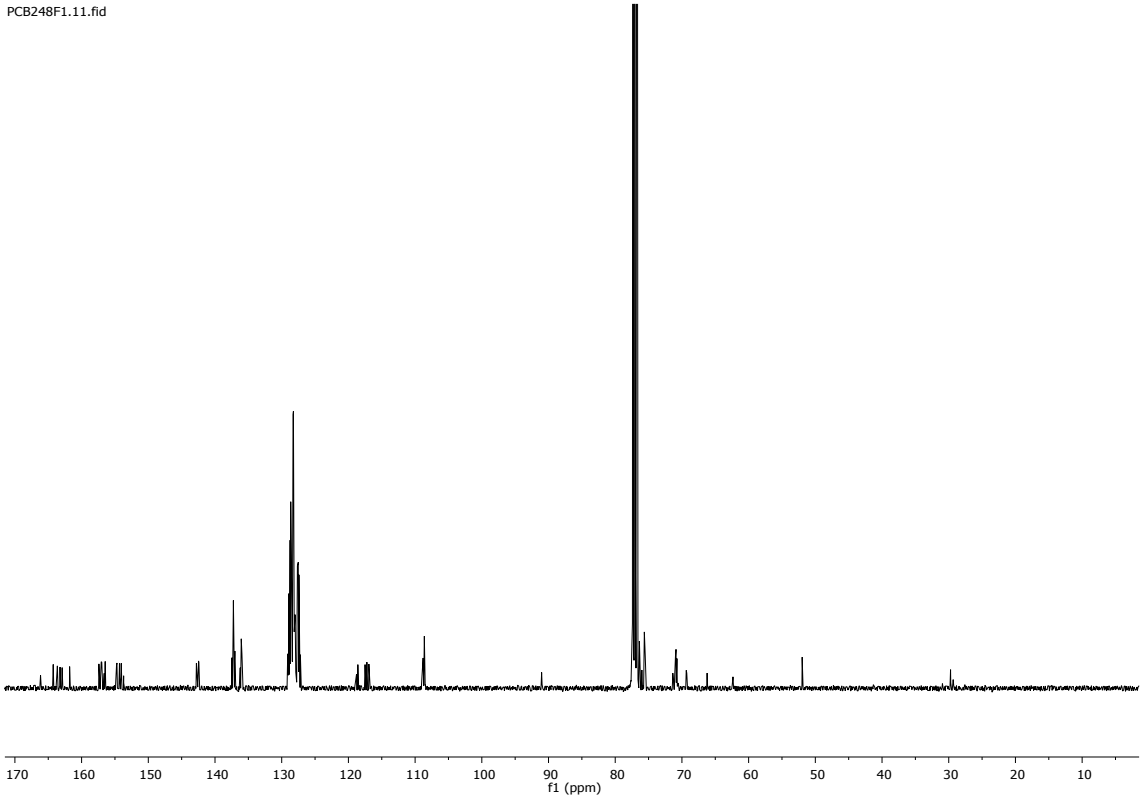

Compound 17 (^{1}H- NMR)

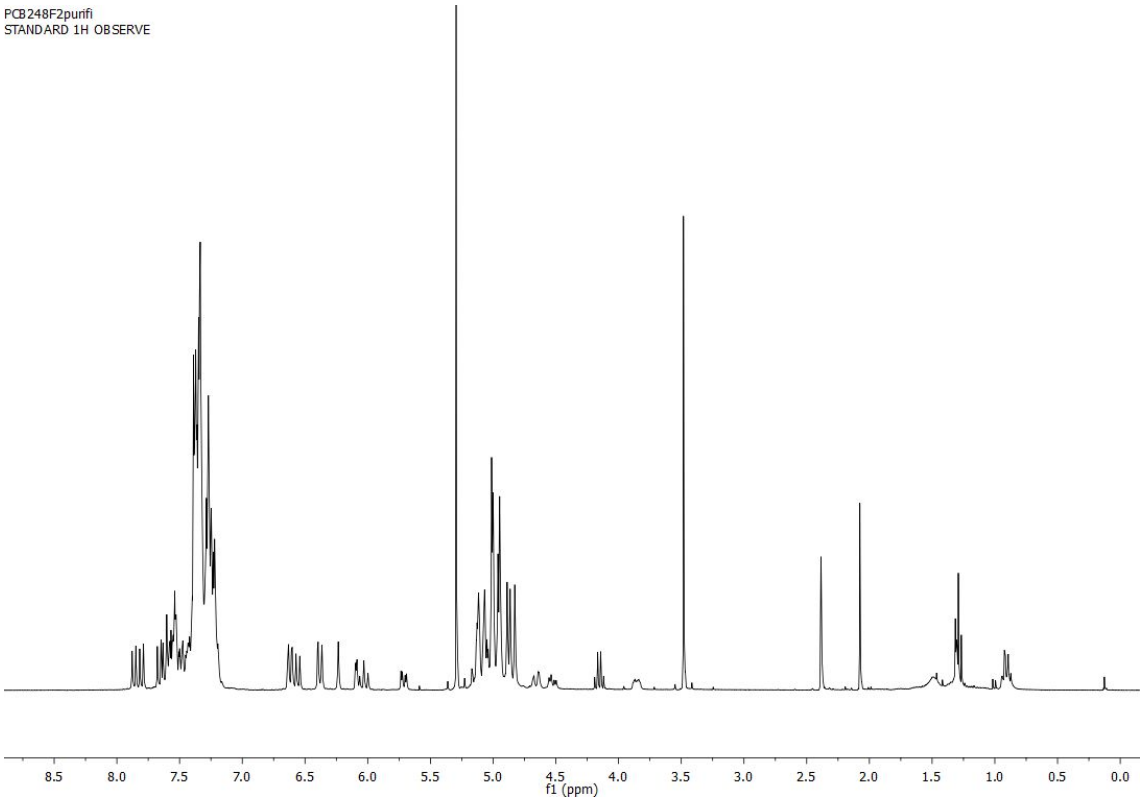

Compound 18 (^{1}H- NMR)

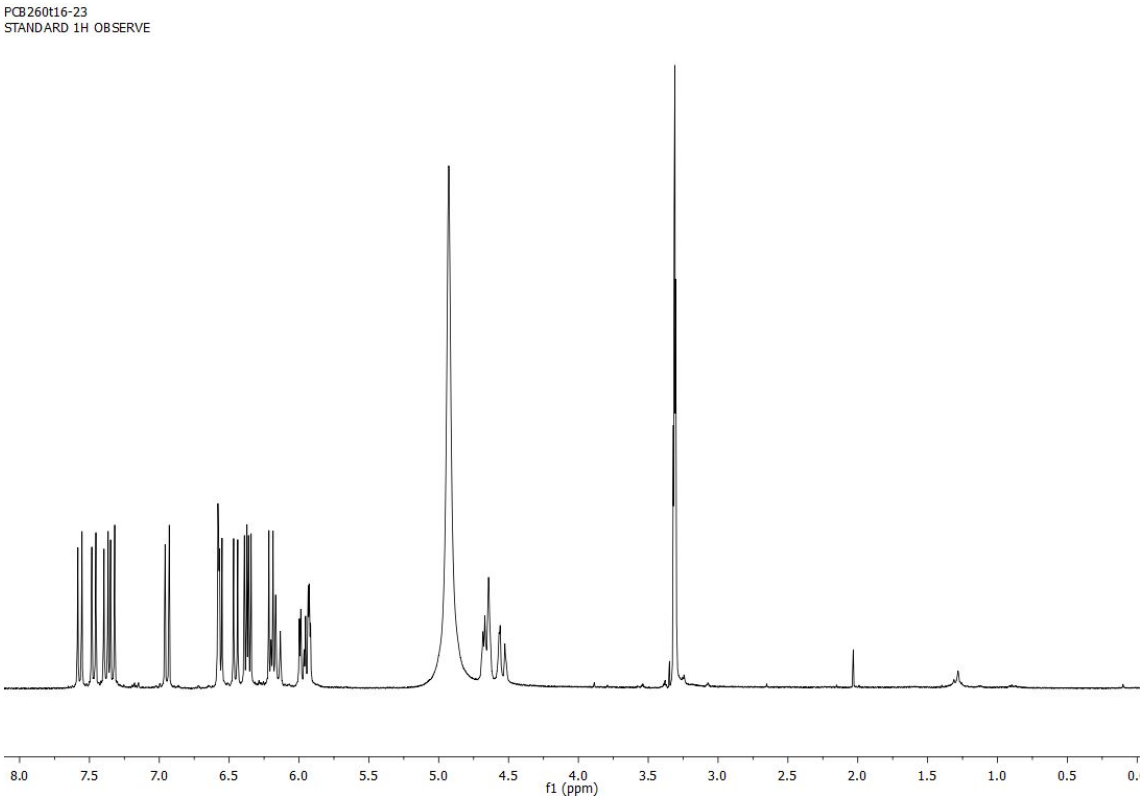

Compound 18 (^{13}C- NMR)

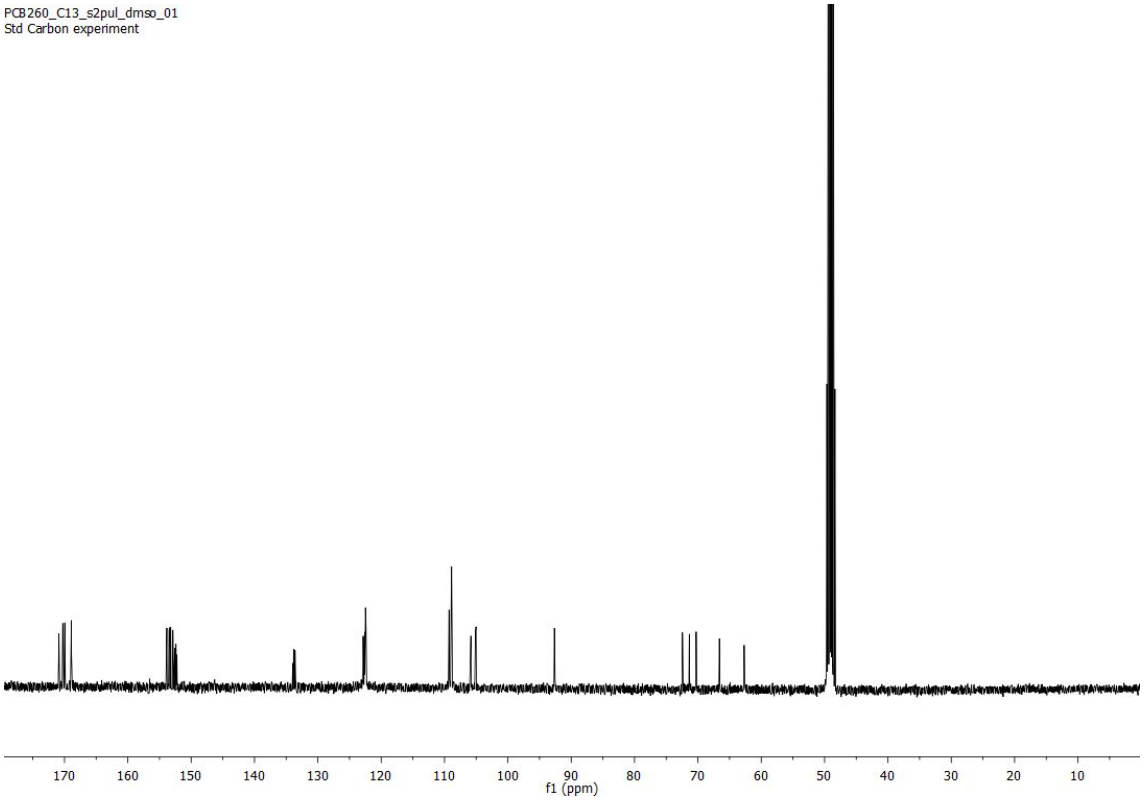

Compound 19 (^{1}H- NMR)

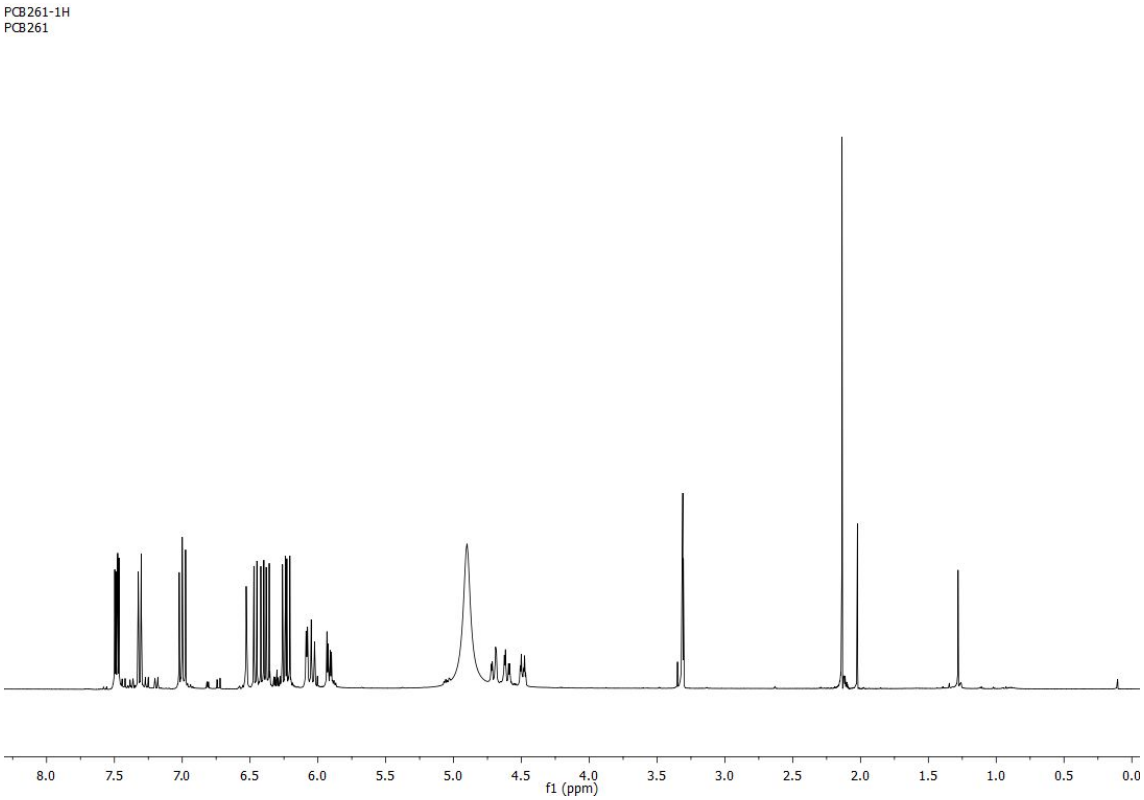

Compound 19 (^{13}C- NMR)

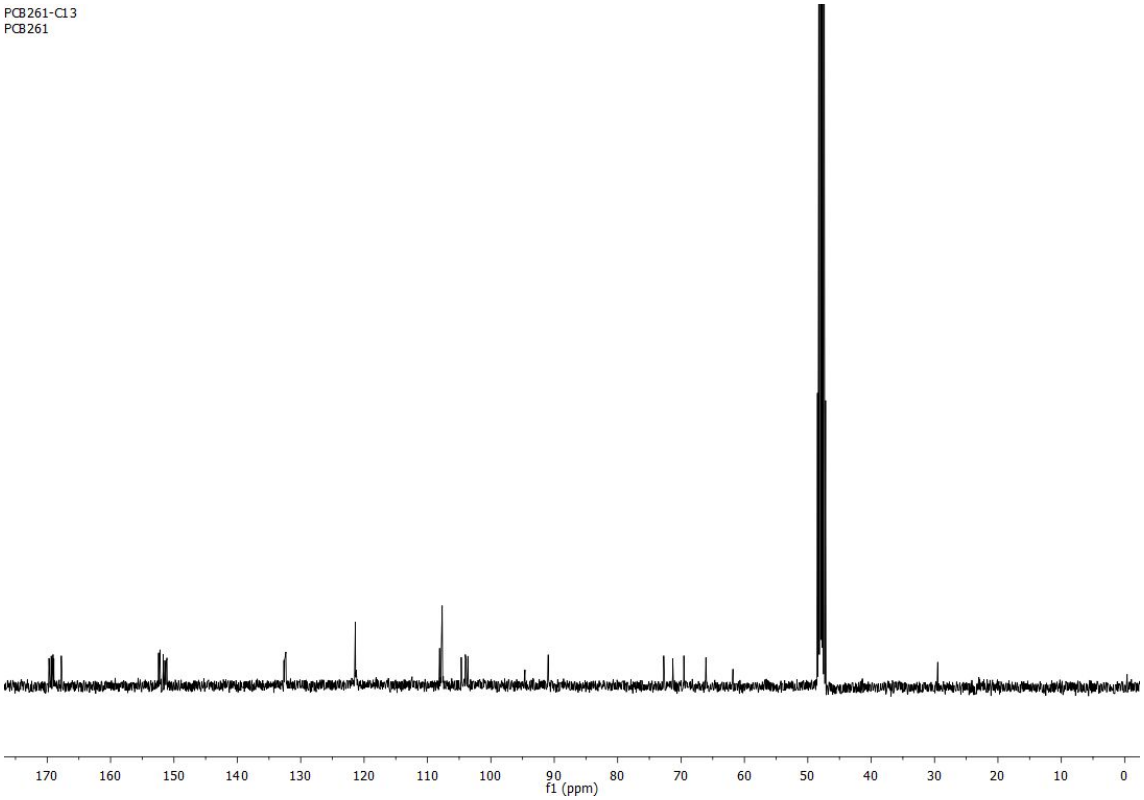

Compound 20 (^{1}H- NMR)

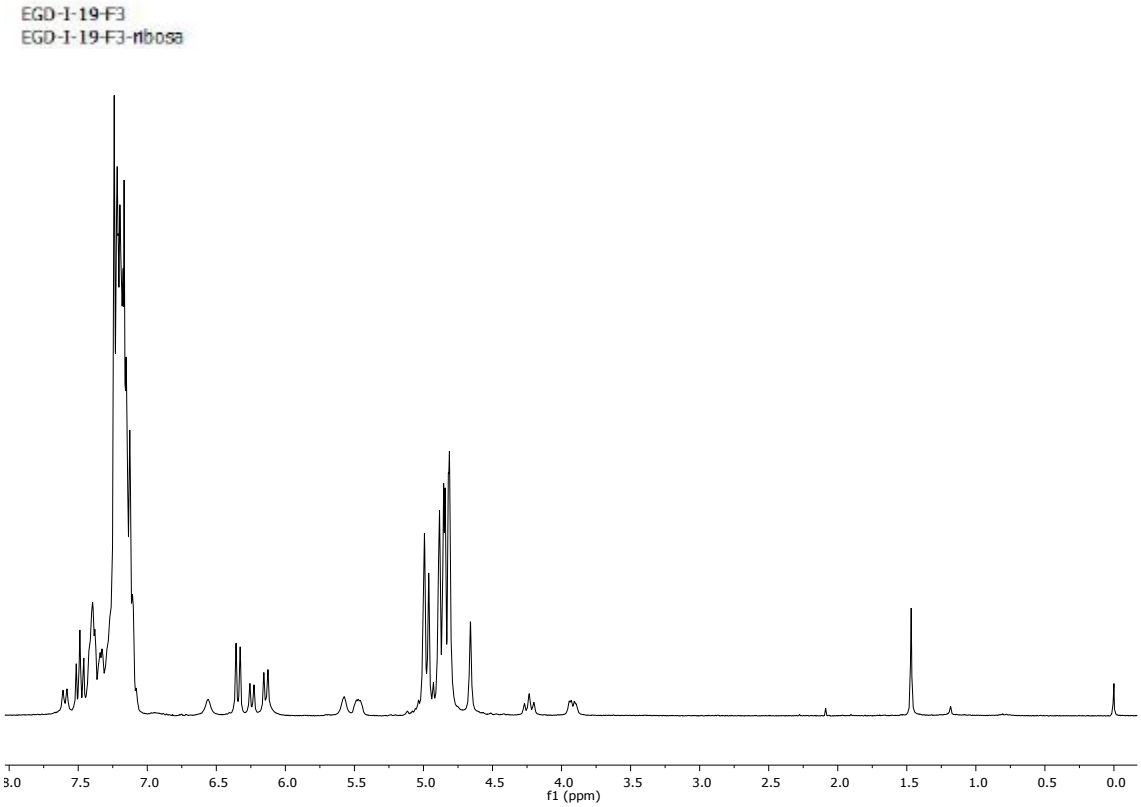

Compound 20 (^{13}C- NMR)

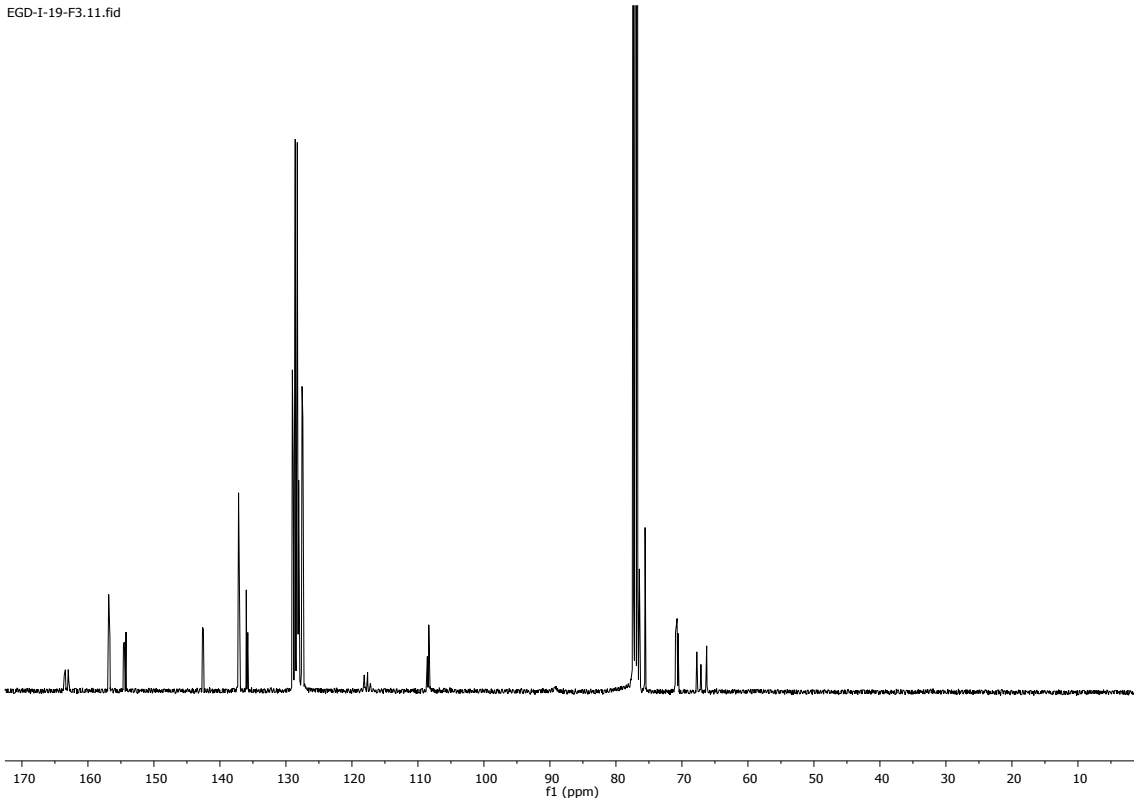

Compound 21 (^{1}H-NMR)

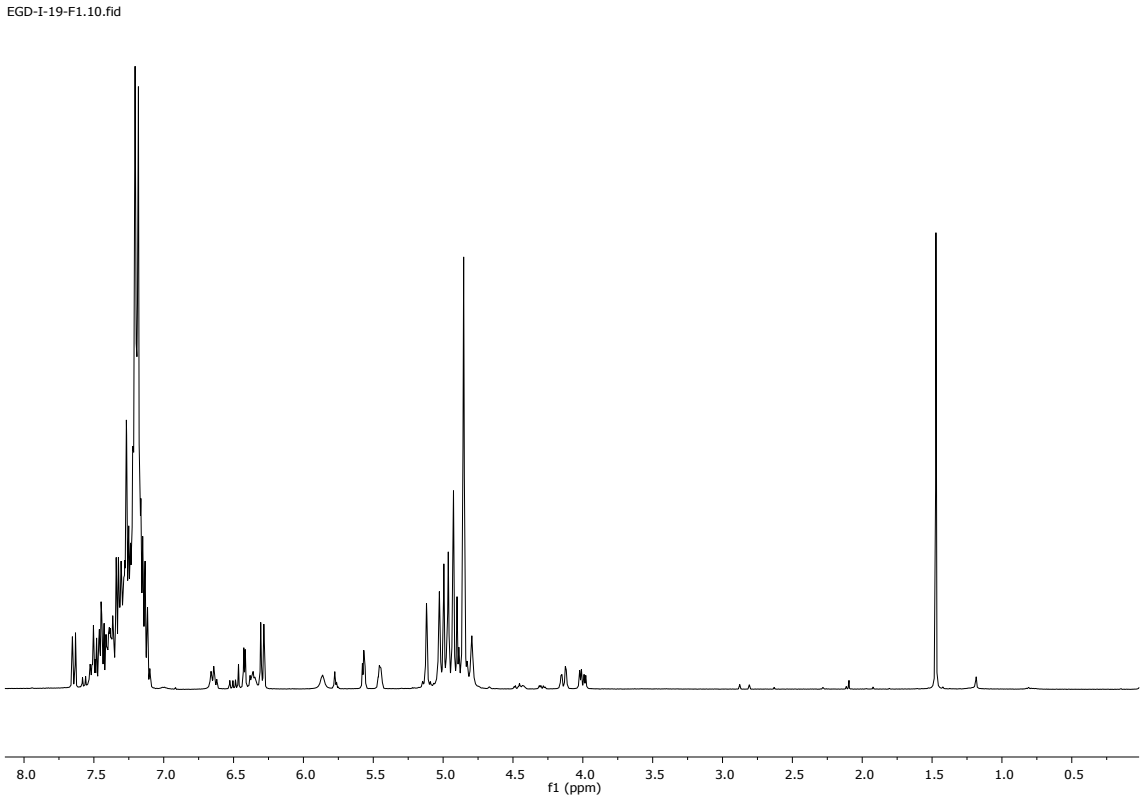

Compound 21 (^{13}C-NMR)

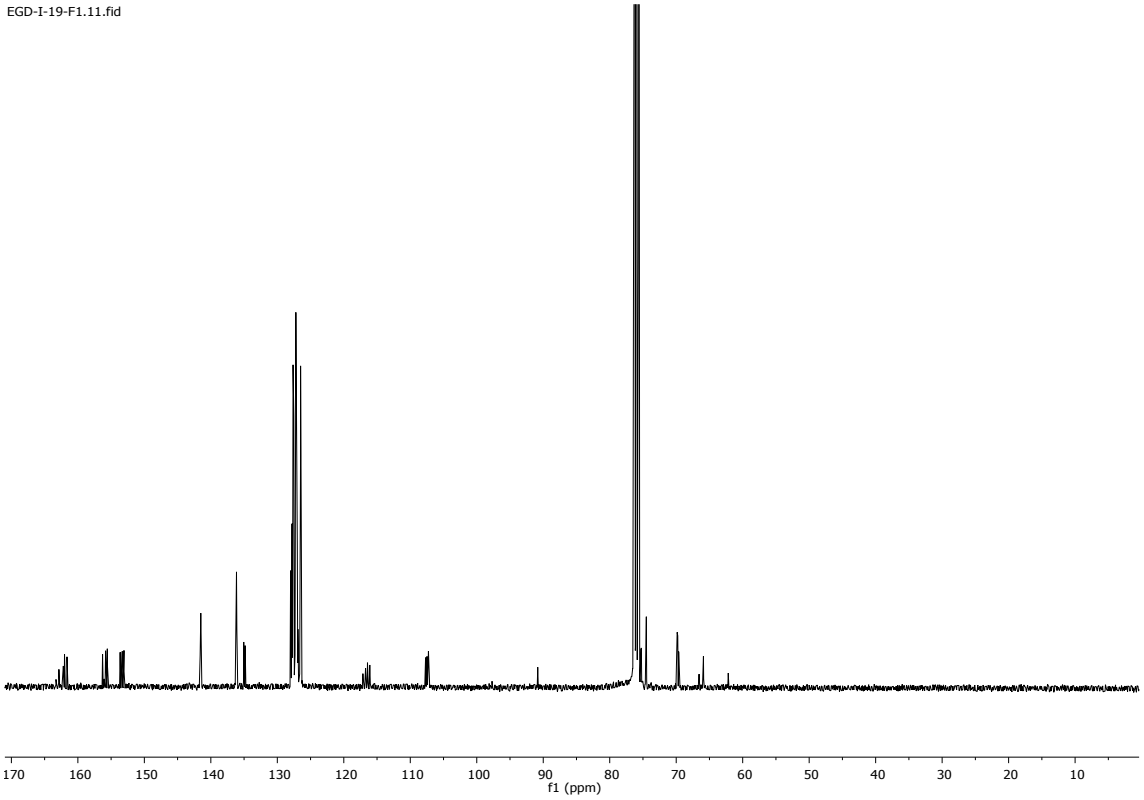

Compound 22 (^{1}H- NMR)

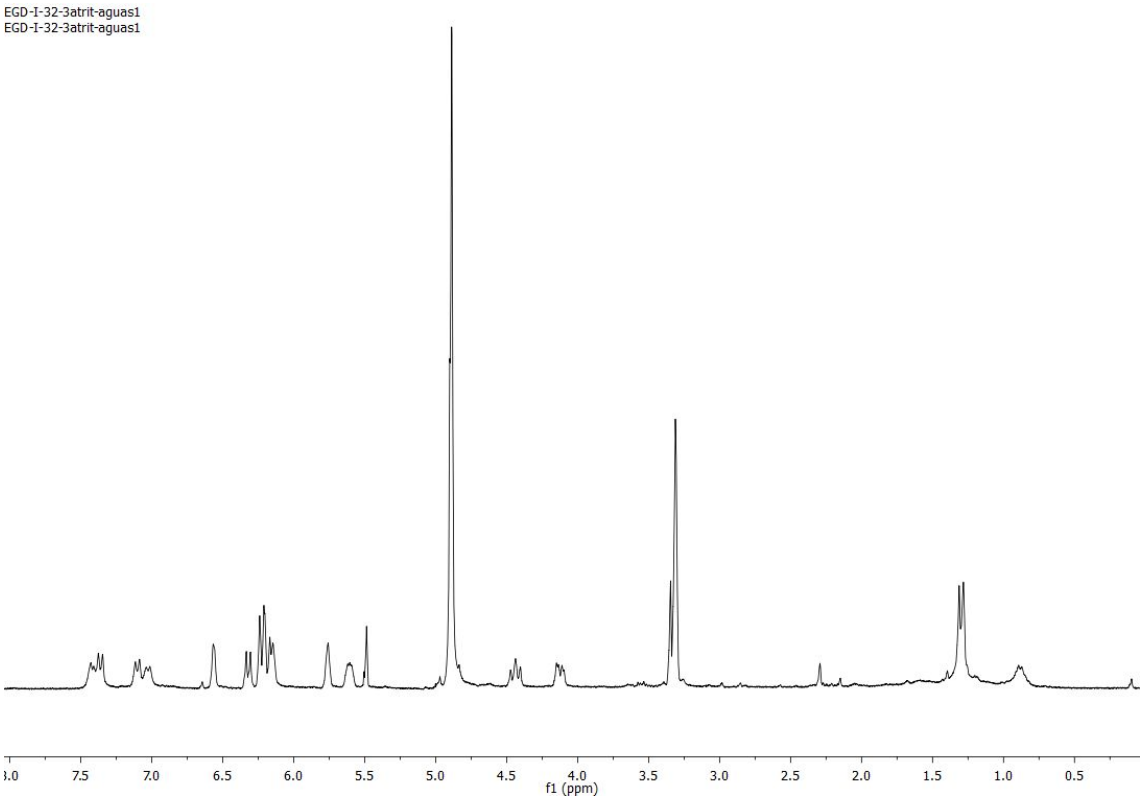

Compound 22 (^{13}C- NMR)

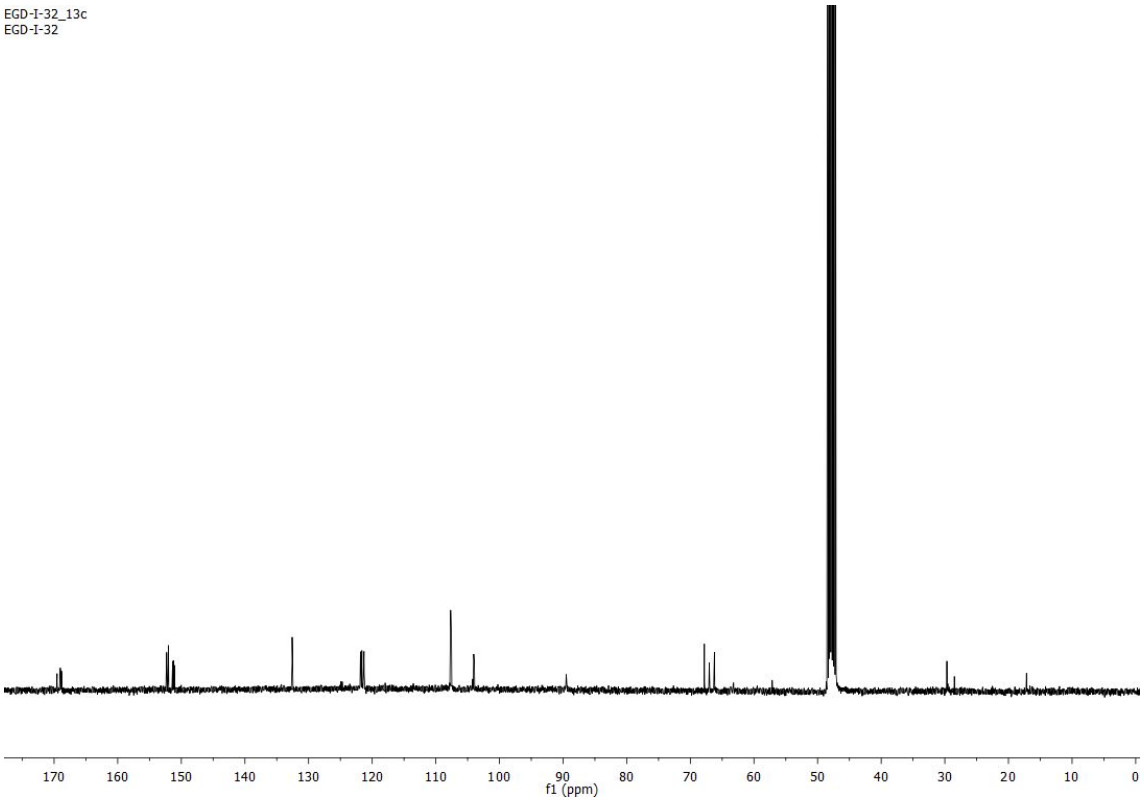

Compound 23 (^{1}H- NMR)

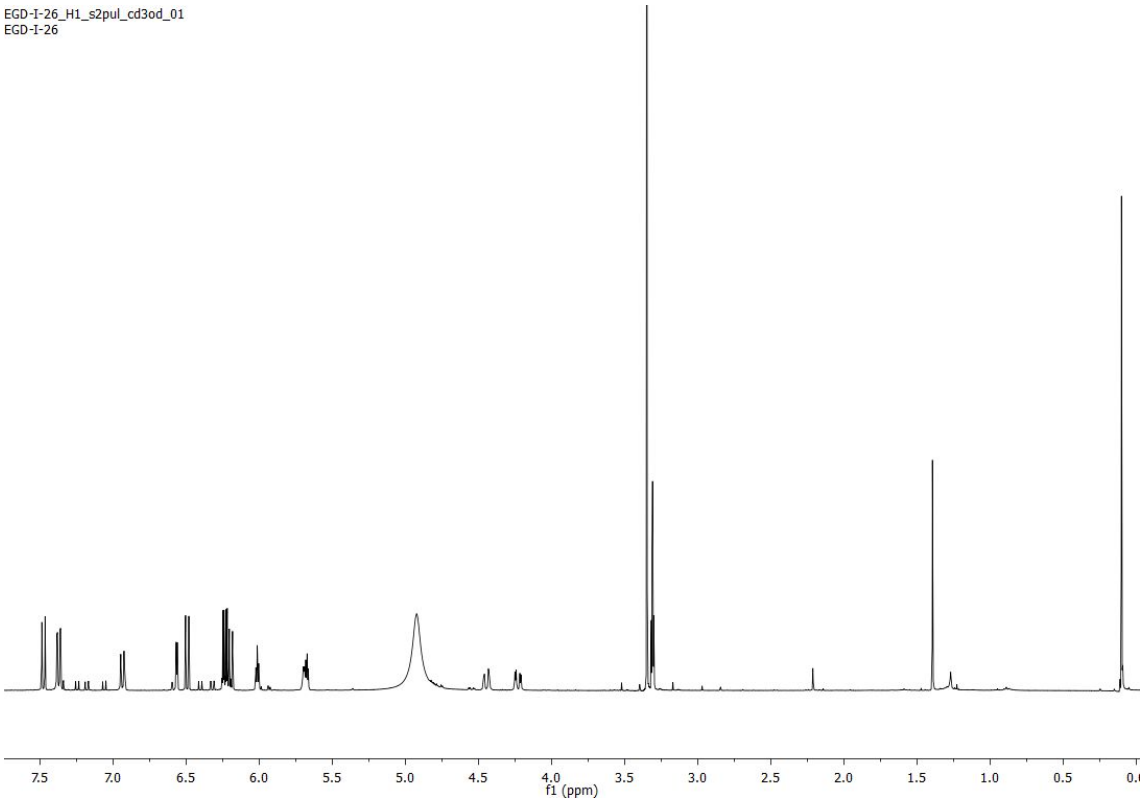

Compound 23 (^{13}C- NMR)

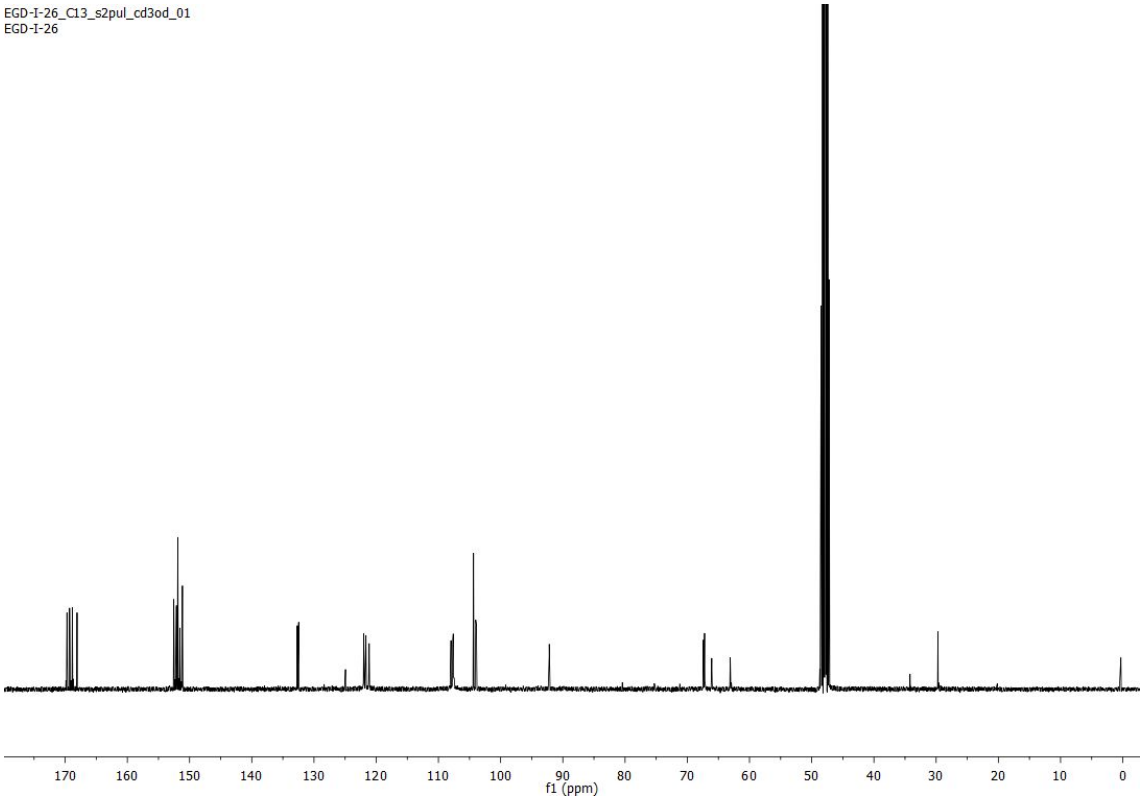

Compound 24 (^{1}H- NMR)

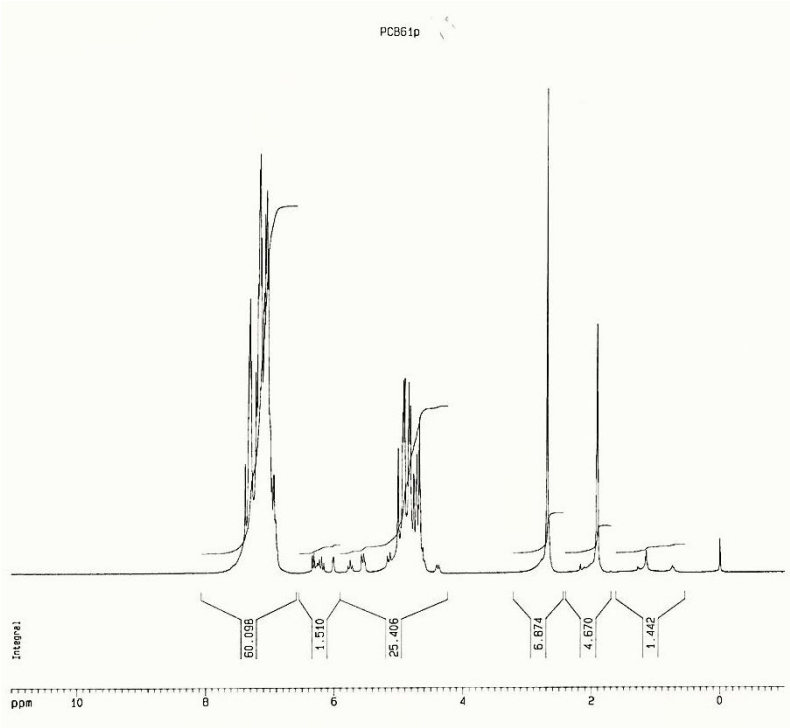

Compound 25 (^{1}H- NMR)

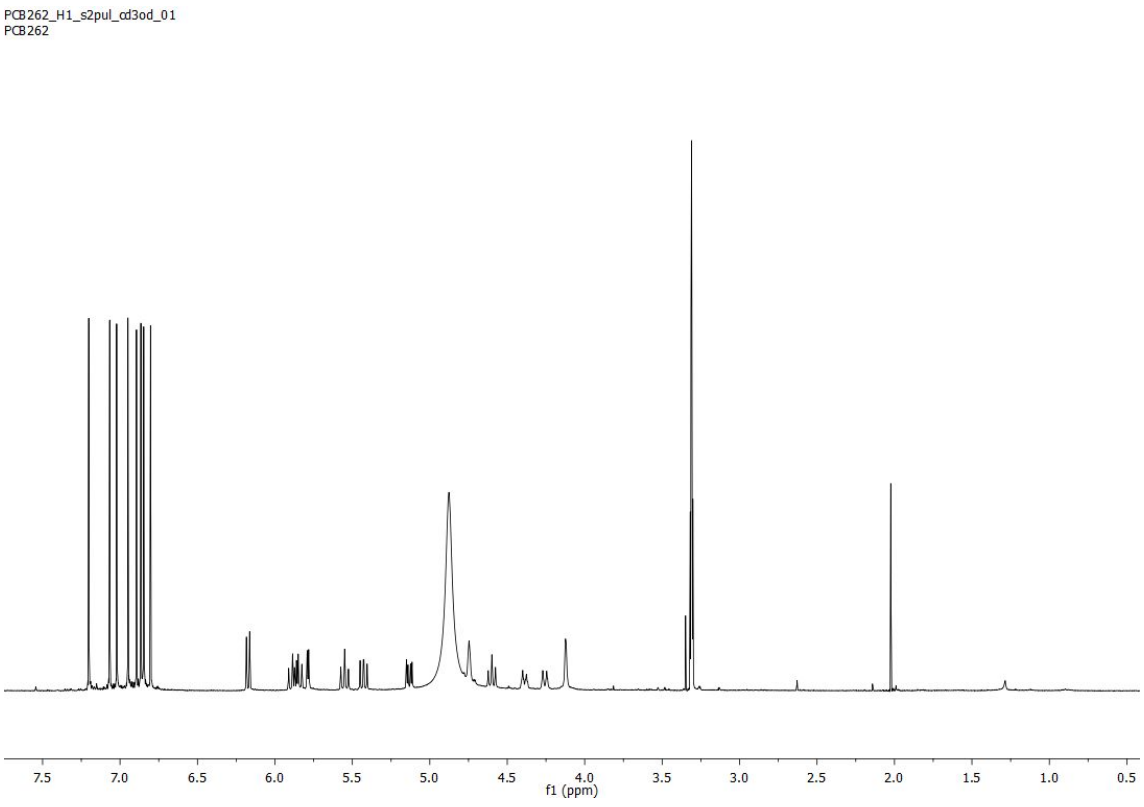

Compound 25 (^{13}C- NMR)

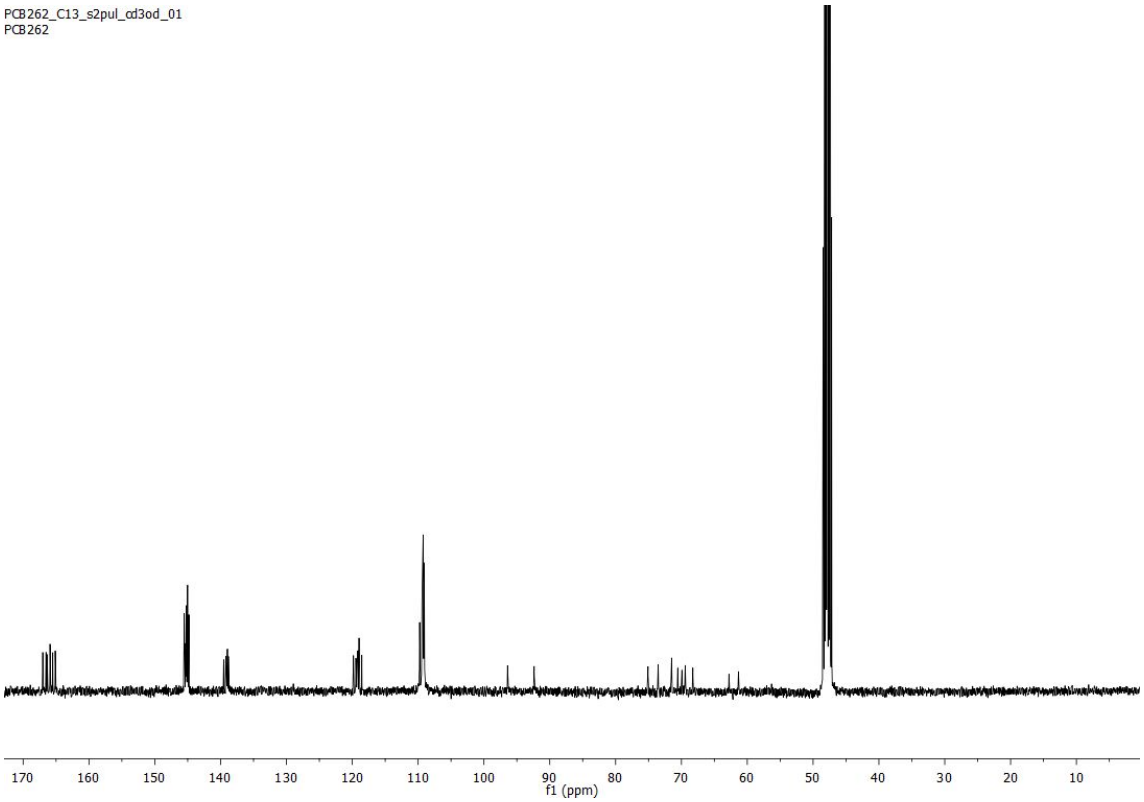

Compound 26 (^{1}H- NMR)

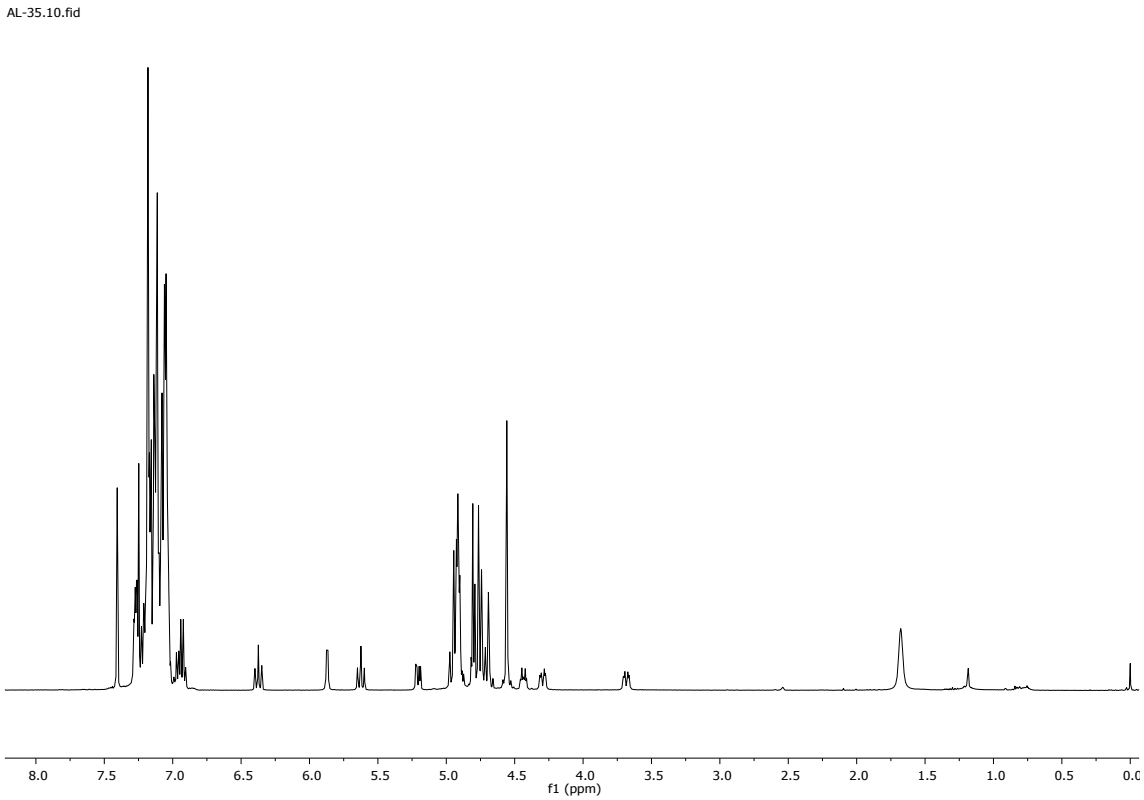

Compound 26 (^{13}C- NMR)

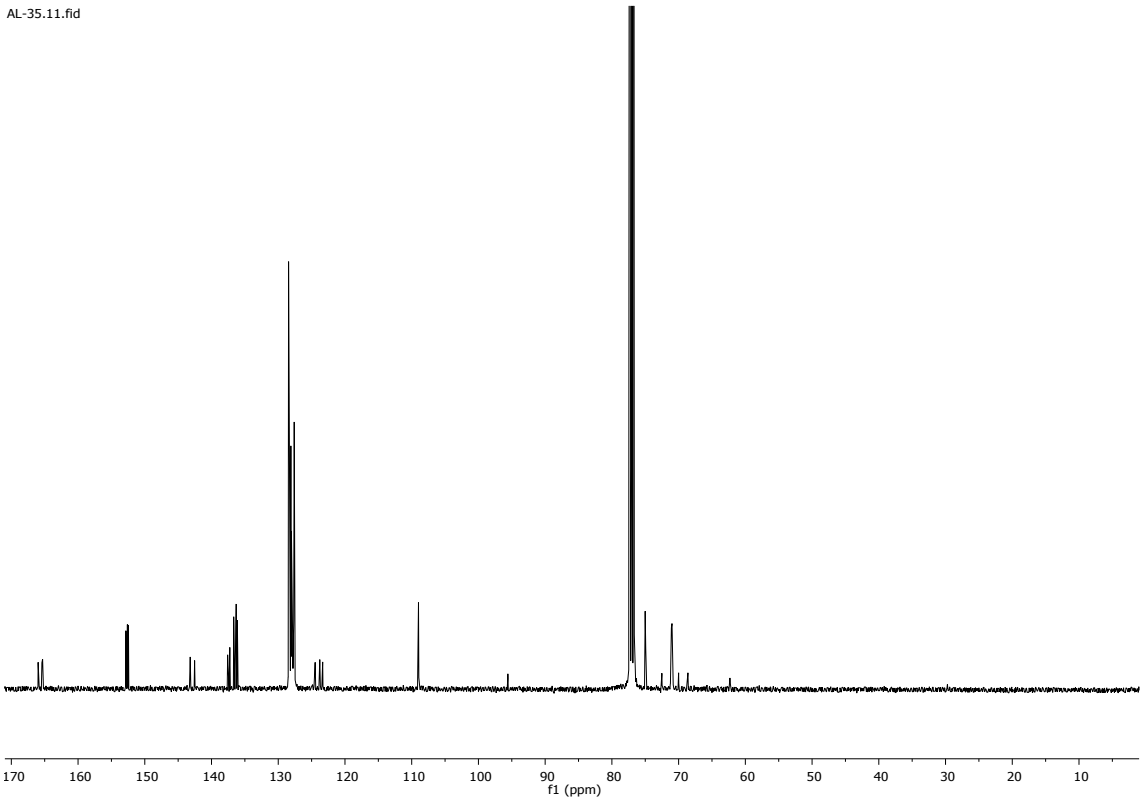

Compound 27 (^{1}H- NMR)

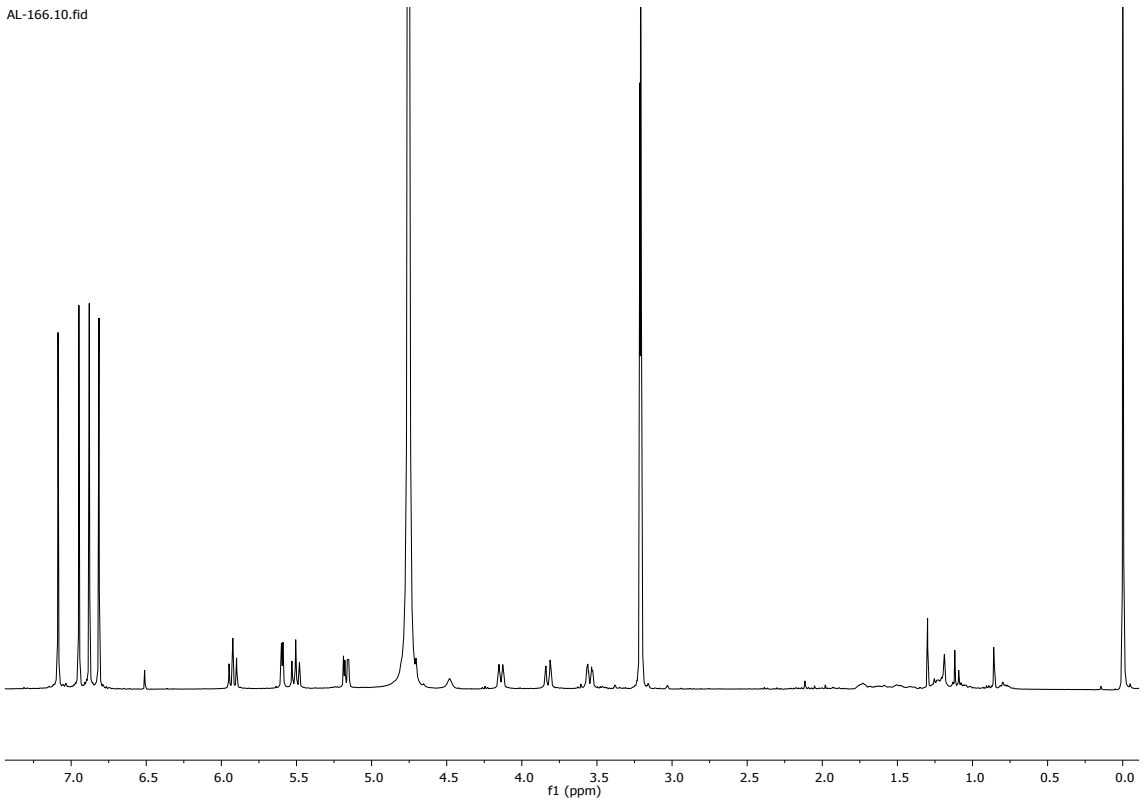

Compound 27 (^{13}C- NMR)

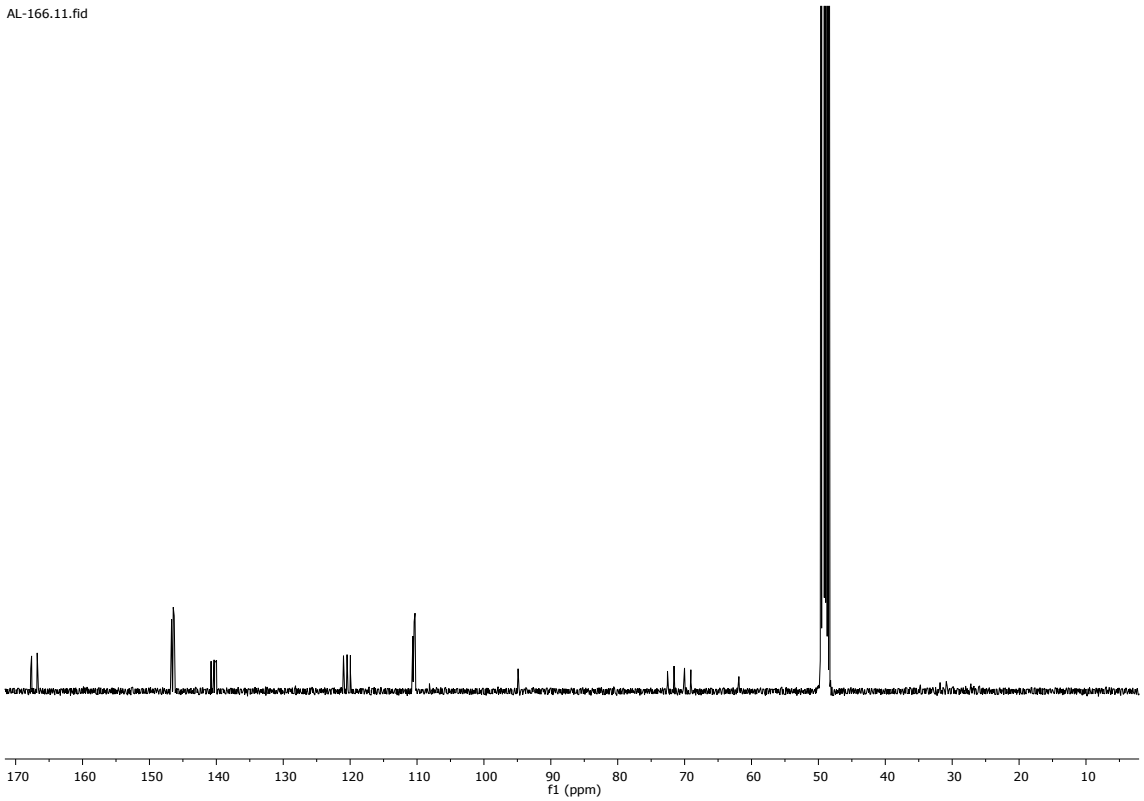

Compound 28 (^{1}H- NMR)

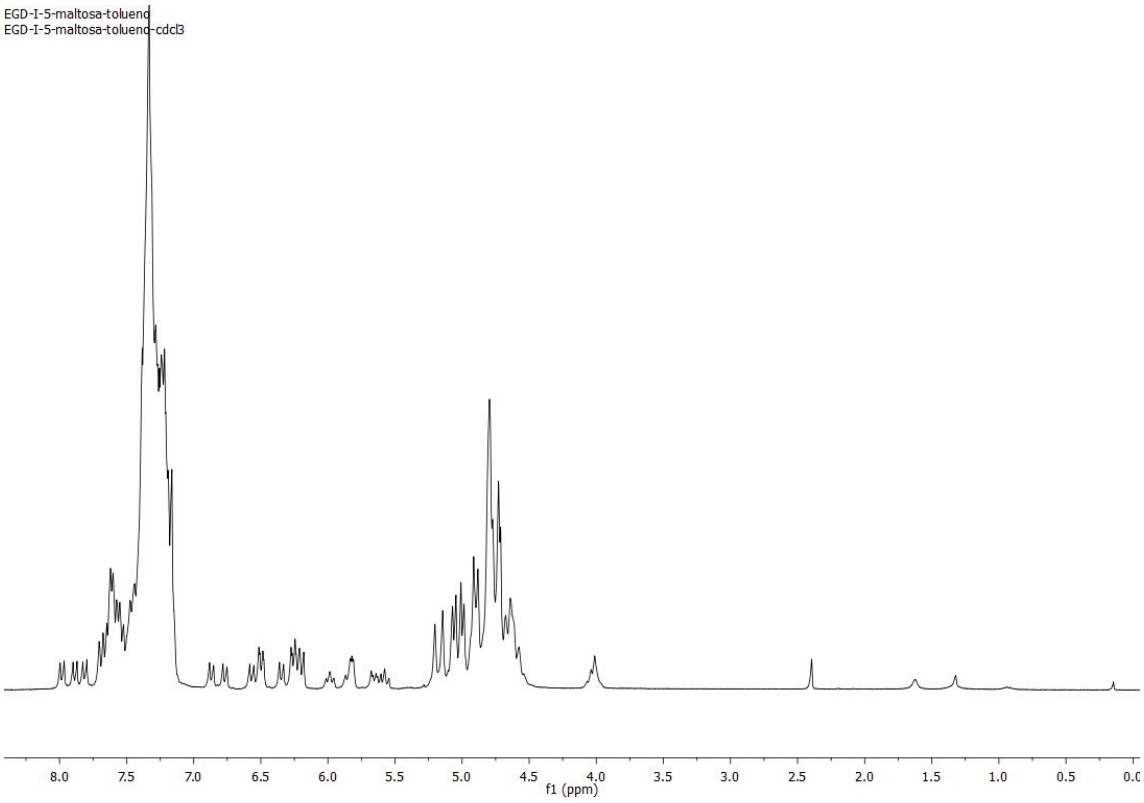

Compound 28 (^{13}C-NMR)

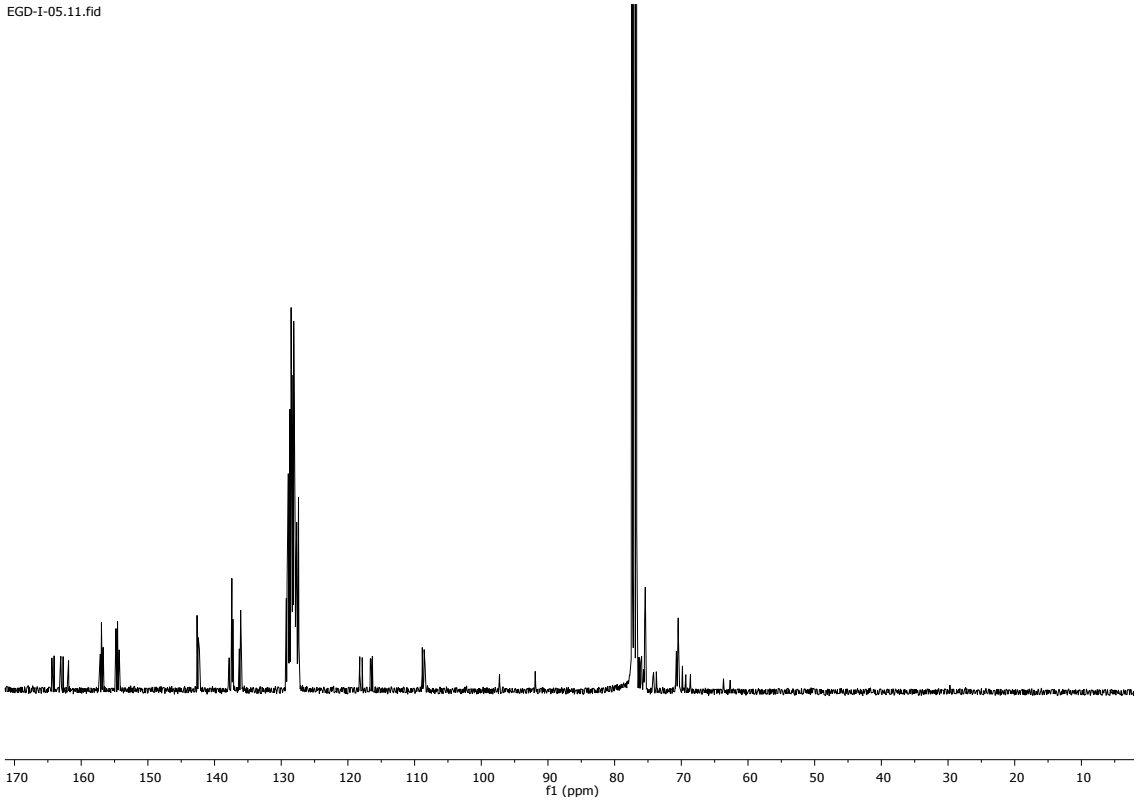

Compound 29 (^{1}H- NMR)

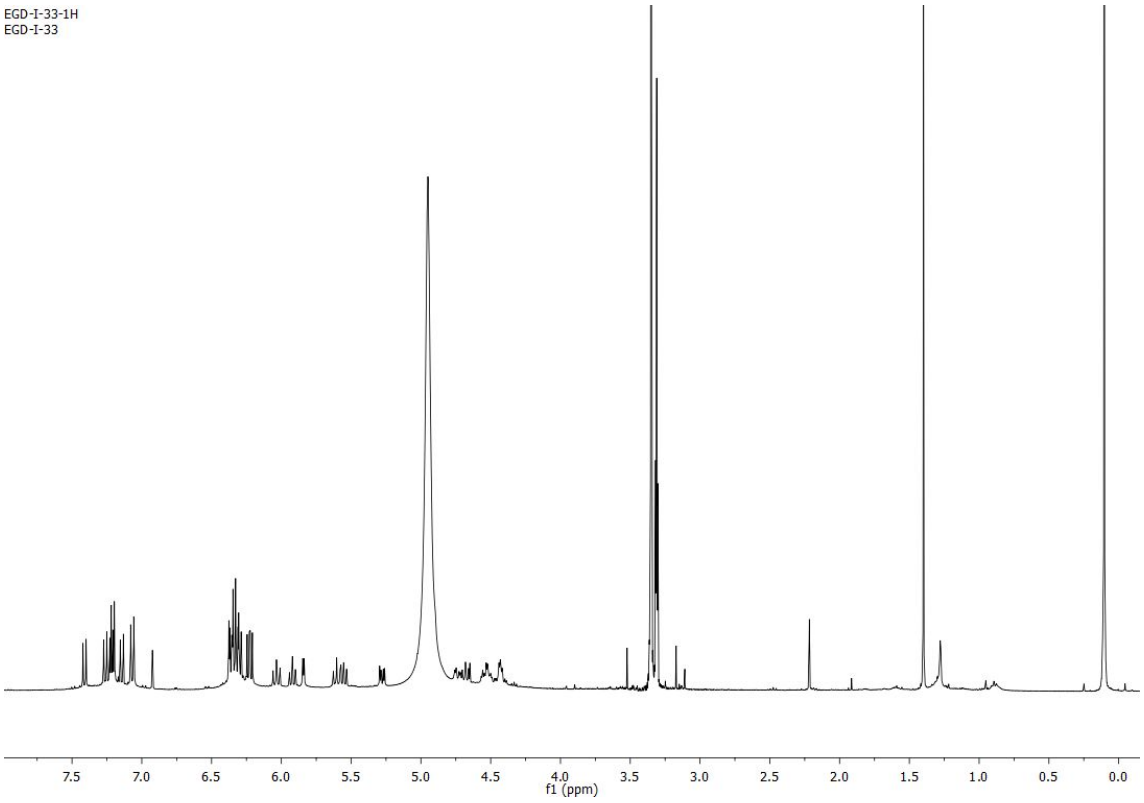

Compound 29 (^{13}C- NMR)

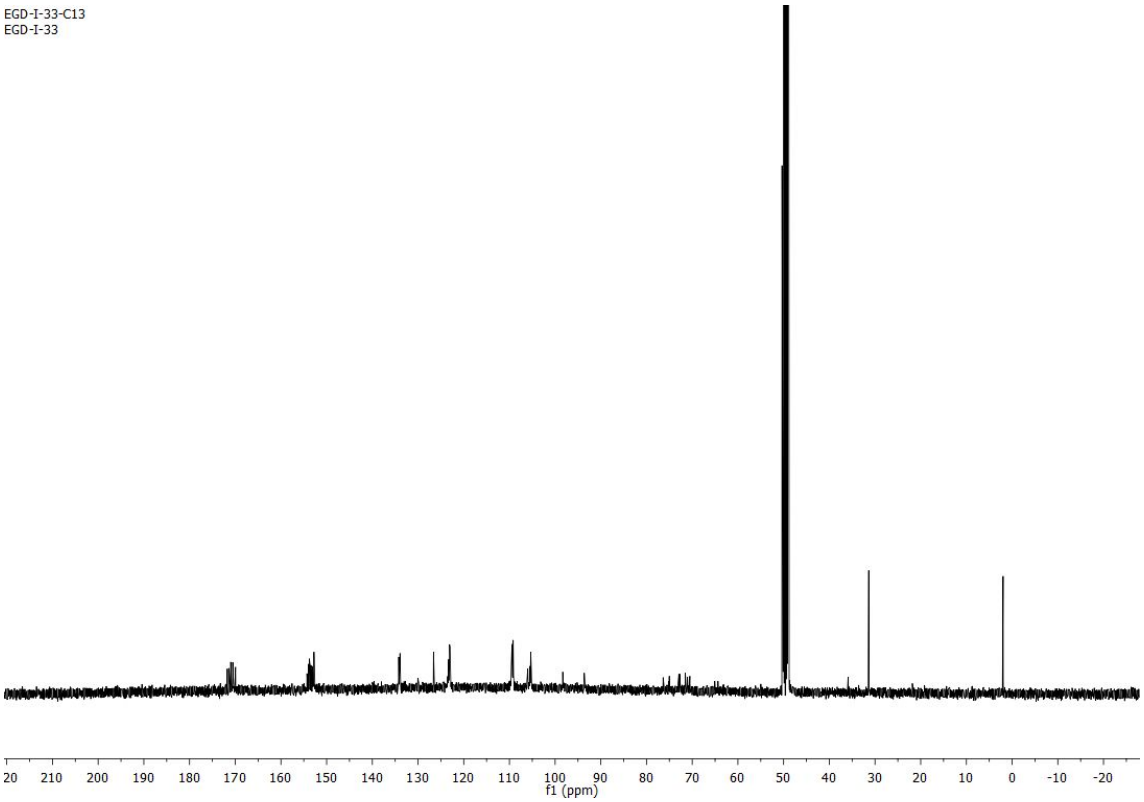

Compound 30 (^{1}H-NMR)

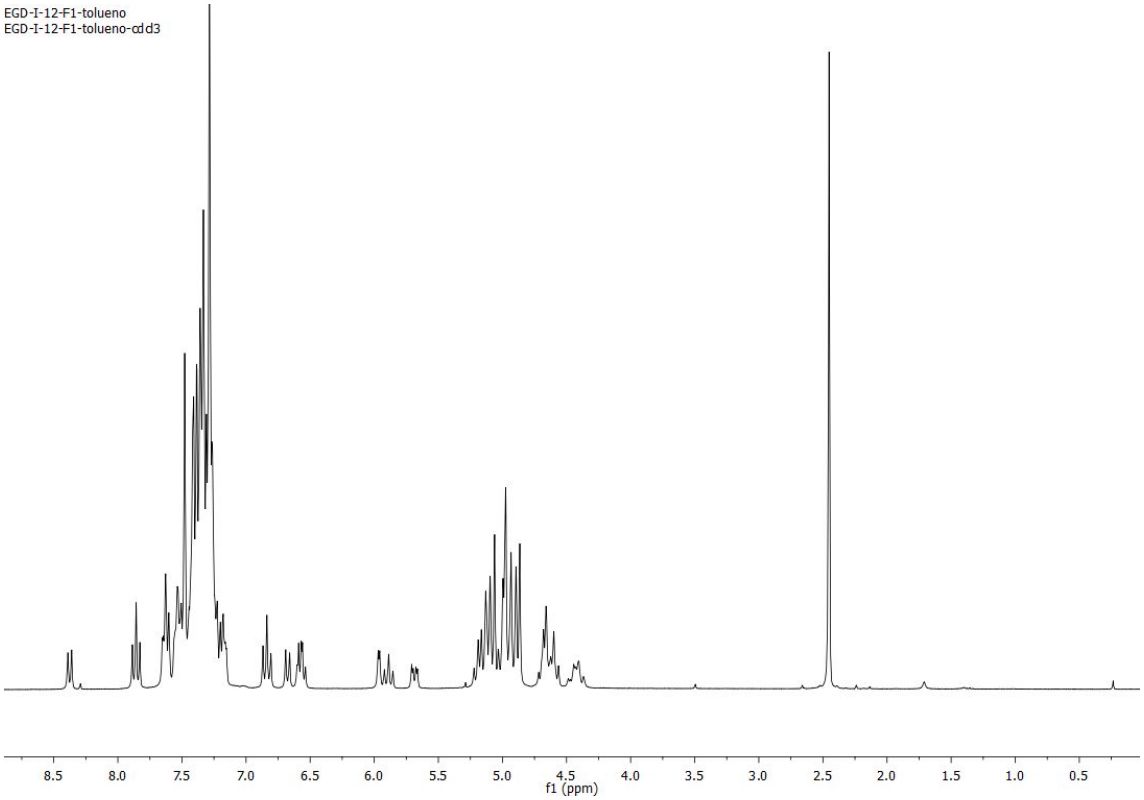

Compound 30 (^{13}C-NMR)

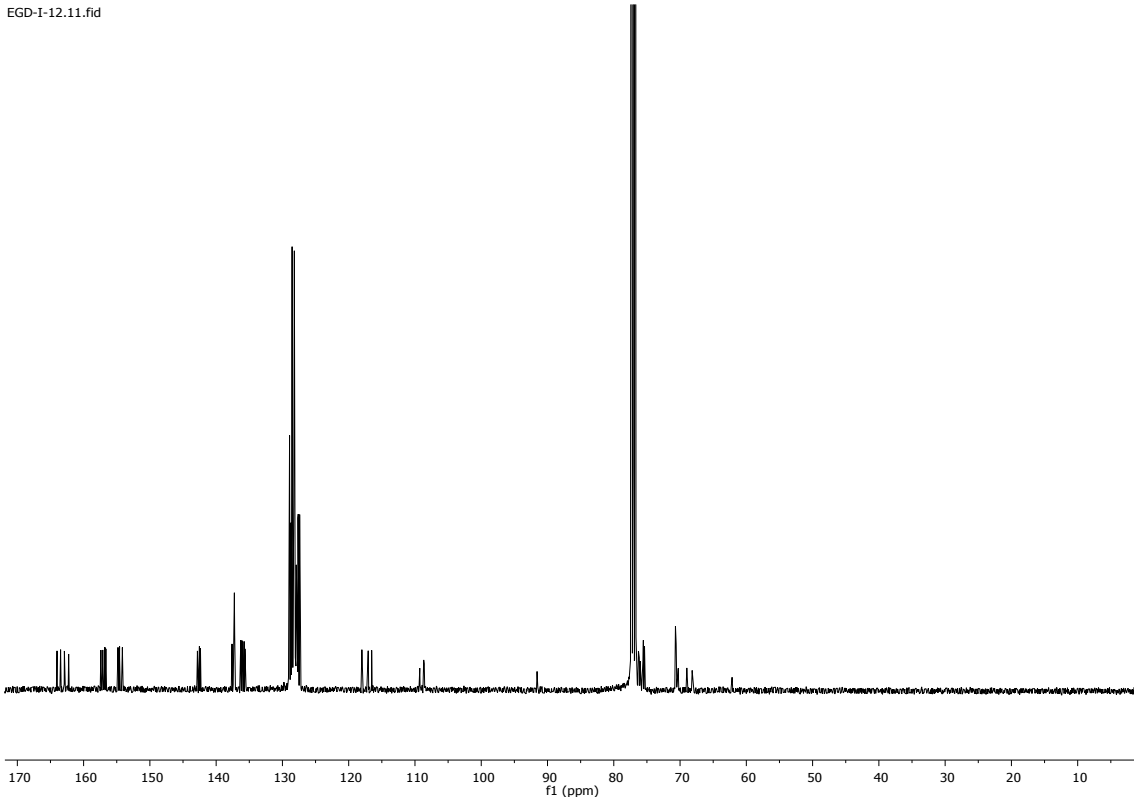

Compound 31 (^{1}H-NMR)

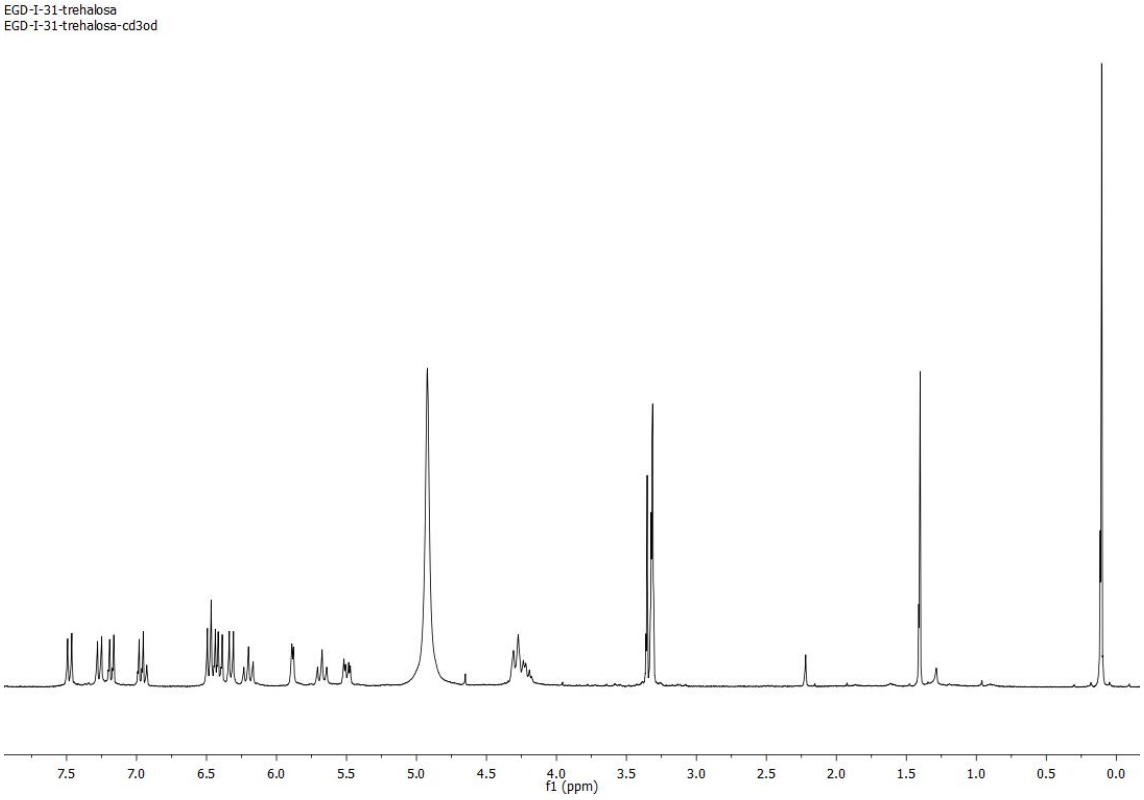

Compound 31 (^{13}C-NMR)

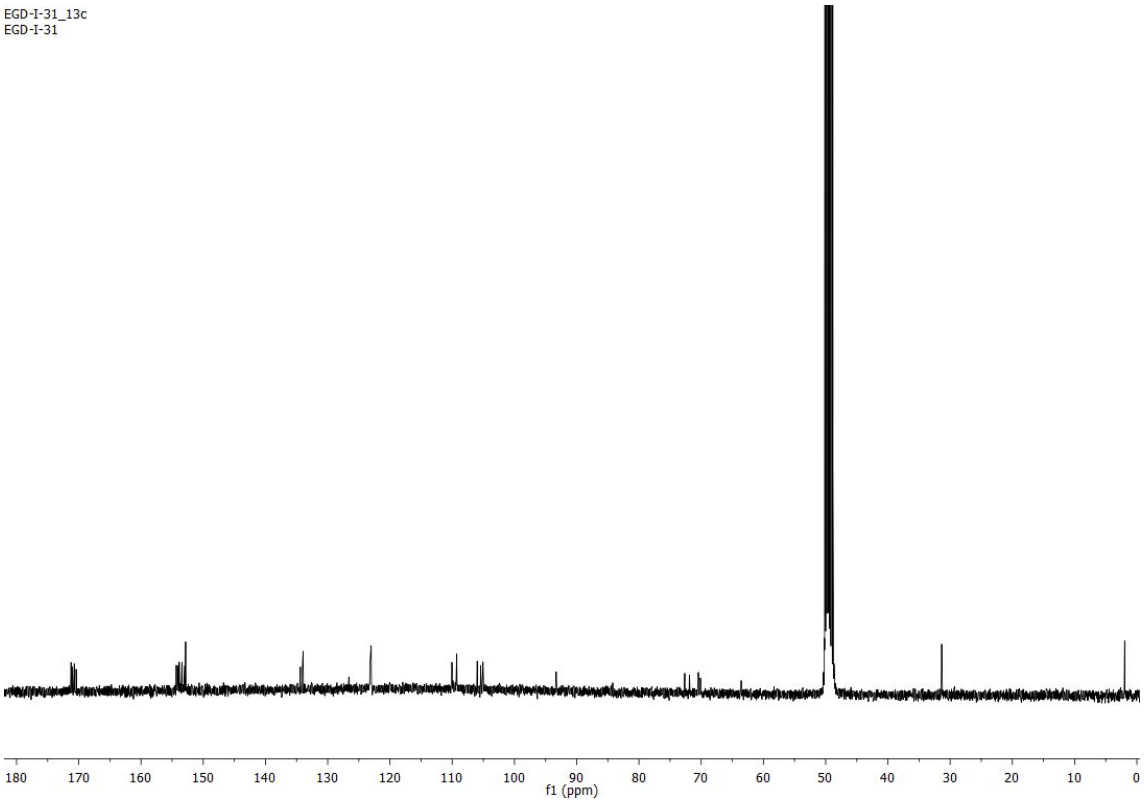

References

1. Ren, Y.; Himmeldirk, K.; Che, X. Synthesis and structure-activity relationship study of antidiabetic penta-*O*-galloyl-D-glucopyranose and its analogues. *J. Med. Chem*. **2006**, *49*, 2829-2837.
2. Duus, J.∅.; Gotfredsen, Ch. H.; Bock, K. Carbohydrate structural determination by NMR spectroscopy: modern methods and limitations, *Chem. Rev.* **2000,** *100*, 4589-4614.
3. Hurd, R.E.; John, B.K. Gradient-Enhanced Proton-Detected Heteronuclear Multiple-Quantum Coherence Spectroscopy, *J. Magn. Reson.* **1991**, *91*, 648-653.
4. Kay, L.E.; Keifer, P.; Saarinen, T. Pure absorption gradient enhanced heteronuclear single quantum correlation spectroscopy with improved sensitivity, *J. Am. Chem. Soc.* **1992**, *114*, 10663-10665.
5. Gola, G; Libenson P.; Gandolfi-Donadío L.; Gallo-Rodriguez C. Synthesis of 2,3,5,6-tetra-*O*-benzyl-D-galactofuranose for α-glycosidation. *Arkivoc* **2005** (xii) 234-242.
6. Decoster E.; Lacombe J.-M.; Strebler J.-L; Ferrari., B.; Pavia, A. *J. Carbohydr. Chem.* **1983**, *2*, 329-341.
7. Bock K.; Pedersen C. Carbon-13 Nuclear Magnetic Resonance Spectroscopy of Monosaccharides, *Adv. Carbohydr. Chem. Biochem.* **1983**, *41*, 27-66.